The EMBO Journal vol.14 no.23 pp.5892–5907, 1995

FKBP12–rapamycin target TOR2 is a vacuolar protein with an associated phosphatidylinositol-4 kinase activity

Maria E.Cardenas[1] and Joseph Heitman[1,2,3,4]

[1]Departments of Genetics and [2]Pharmacology and the [3]Howard Hughes Medical Institute, Duke University Medical Center, Box 3546, Durham, NC 27710, USA

[4]Corresponding author

In complex with the immunophilin FKBP12, the natural product rapamycin inhibits signal transduction events required for G_1 to S phase cell cycle progression in yeast and mammalian cells. Genetic studies in yeast first implicated the TOR1 and TOR2 proteins as targets of the FKBP12–rapamycin complex. We report here that the TOR2 protein is membrane associated and localized to the surface of the yeast vacuole. Immunoprecipitated TOR2 protein contains readily detectable phosphatidylinositol-4 (PI-4) kinase activity attributable to either a TOR2 intrinsic activity or to a PI-4 kinase tightly associated with TOR2. Importantly, we find that rapamycin stimulates FKBP12 binding to wild-type TOR2 but not to a rapamycin-resistant TOR2-1 mutant protein. Surprisingly, FKBP12–rapamycin binding does not markedly inhibit the PI kinase activity associated with TOR2, but does cause a delocalization of TOR2 from the vacuolar surface, which may deprive the TOR2-associated PI-4 kinase activity of its *in vivo* substrate. Several additional findings indicate that vacuolar localization is important for TOR2 function and, conversely, that TOR2 modulates vacuolar morphology and segregation. These studies demonstrate that TOR2 is an essential, highly conserved component of a signal transduction pathway regulating cell cycle progression conserved from yeast to man.

Keywords: FKBP12/phosphatidylinositol/rapamycin/TOR2/vacuolar protein

Introduction

Cyclosporin A (CsA), FK506 and rapamycin are natural products with potent antifungal and immunosuppressive activity via their ability to inhibit signal transduction (Heitman *et al.*, 1992; Schreiber and Crabtree, 1992; Cardenas *et al.*, 1994a). CsA is a cyclic peptide and FK506 and rapamycin are structurally related macrolides. These compounds suppress the immune system by inhibiting T-cell function. CsA and FK506 prevent T-cell activation by antigen presentation, whereas rapamycin blocks T-cell responses to interleukin-2 (Dumont *et al.*, 1990a,b; Mattila *et al.*, 1990). In addition, rapamycin inhibits proliferation in response to a variety of other growth factors in many mammalian cell types (Chung *et al.*, 1992; Price *et al.*, 1992; Albers *et al.*, 1993; Jayaraman and Marks, 1993; de Groot *et al.*, 1994; Dilling *et al.*, 1994). In both yeast and mammalian cells, the actions of FK506 and rapamycin are mediated by association with a highly conserved protein, the *cis–trans* peptidyl-prolyl isomerase FKBP12 (Bierer *et al.*, 1990; Dumont *et al.*, 1990a,b; Heitman *et al.*, 1991a,b; Foor *et al.*, 1992; Breuder *et al.*, 1994). Thus, FK506 and rapamycin harness FKBP12 to inhibit components of different signaling cascades.

The target of the FKBP12–FK506 complex, and also of the cyclophilin A–CsA complex, is a calcium–calmodulin-regulated protein phosphatase, calcineurin, which is highly conserved from yeast to mammals (Cyert *et al.*, 1991; J.Liu *et al.*, 1991, 1992; Y.Liu *et al.*, 1991; Ye and Bretscher, 1992). Calcineurin is required to transduce signals in T cells for response to antigen presentation (Clipstone and Crabtree, 1992; O'Keefe *et al.*, 1992), and in yeast cells for recovery from pheromone arrest, cation resistance and, in some strains, viability (Cyert *et al.*, 1991; Foor *et al.*, 1992; Nakamura *et al.*, 1993; Breuder *et al.*, 1994; Cardenas *et al.*, 1995). However, calcineurin is not inhibited by the FKBP12–rapamycin complex.

Several observations reveal that the FKBP12–rapamycin complex inhibits a calcineurin-independent signaling cascade regulating cell cycle progression that is conserved from yeast to man. First, rapamycin is toxic to yeast strains in which calcineurin is not essential (Heitman *et al.*, 1991a). Second, FKBP12 is dispensable for viability but required for rapamycin toxicity in yeast, consistent with the model that the protein–drug complex is toxic (Heitman *et al.*, 1991a). Third, FK506 antagonizes rapamycin action in yeast and in T cells (Bierer *et al.*, 1990; Heitman *et al.*, 1991a). Fourth, FKBP12–rapamycin imposes a specific cell cycle arrest and prevents G_1 to S phase progression in yeast and in T cells (Dumont *et al.*, 1990a,b; Heitman *et al.*, 1991a). Lastly, human FKBP12 complements yeast strains lacking yeast FKBP12, indicating that the human FKBP12–rapamycin complex can inhibit the yeast target of FKBP12–rapamycin (Koltin *et al.*, 1991).

Genetic studies in yeast first implicated the *TOR* gene products as targets of the FKBP12–rapamycin complex (Heitman *et al.*, 1991a). Mutations in the *TOR1* or *TOR2* genes protect yeast cells from the toxic effects of rapamycin (Heitman *et al.*, 1991a). The observation of non-allelic non-complementation between FKBP12, TOR1 and TOR2 mutations led to the proposal that TOR1 and TOR2 are the direct physical targets of the FKBP12–rapamycin complex (Heitman *et al.*, 1991a, 1992). Analysis of the cloned *TOR1* and *TOR2* genes revealed the potential to encode large ~280 kDa proteins which share 67% identity with each other (Cafferkey *et al.*, 1993; Kunz *et al.*, 1993; Helliwell *et al.*, 1994). By gene disruption, *TOR2* is essential whereas *TOR1* is not.

The carboxy-terminal regions of both TOR1 and TOR2 share significant identity with several proteins with phos-

phatidylinositol kinase activity, including the 110 kDa subunit of mammalian phosphatidylinositol-3 (PI-3) kinase (Hiles *et al.*, 1992), the yeast VPS34 PI-3 kinase (Schu *et al.*, 1993) and yeast and human PI-4 kinases (Flanagan *et al.*, 1993; Garcia-Bustos *et al.*, 1994; Wong and Cantley, 1994; Yoshida *et al.*, 1994). In addition, biochemical studies have recently identified mammalian proteins that associate with the FKBP12–rapamycin complex and which share significant similarity to the yeast TOR proteins and PI kinases (Brown *et al.*, 1994; Sabatini *et al.*, 1994).

The role of PI metabolites in signal transduction has been well established in several cases (reviewed in Berridge and Irvine, 1989; Majerus *et al.*, 1990; Berridge, 1993; Janmey, 1994, 1995). For example, the combined action of a PI-4 kinase and a PI4P-specific PI-5 kinase generates the lipid precursor PI4,5P_2, which is subsequently cleaved by phospholipase C (PLC) to generate the second messengers diacylglycerol (DAG), which activates PKC, and I1,4,5P_3, a water-soluble second messenger that triggers release of intracellular calcium stores via the IP_3 receptor (see Berridge, 1993). In other cases, novel roles for PI metabolites in signaling are emerging but are less well established. For example, cleavage of the lipid precursor PI4P by PLC generates I1,4P_2, another water-soluble molecule which can activate DNA polymerase α *in vitro* and may be required for progression into S phase *in vivo* (Sylvia *et al.*, 1988; York *et al.*, 1994). In mammalian cells, the 110 kDa catalytic subunit of PI-3 kinase is recruited and activated by a number of growth factor receptors and can generate a class of distinct phospholipids (PI3P, PI3,4P_2 and PI3,4,5P_3) that are immune to cleavage by PLC and are likely to act directly as lipid second messengers (reviewed by Janmey, 1994, 1995; Kapeller and Cantley, 1994). Although a number of proteins have been identified which bind these phospholipids, the relevant *in vivo* targets remain to be established. Recent studies on the yeast VPS34 protein, a novel PI-3 kinase, have revealed a role for PI metabolites in intracellular protein sorting and transport of vesicles between different compartments of the secretory pathway (Schu *et al.*, 1993; Stack *et al.*, 1993). Recent findings have also established a role for PI metabolites, a PI transfer protein, and a PI4P-5 kinase in calcium-activated secretion in PC12 cells (Hay *et al.*, 1995). The complexity of the metabolic pathways for PI and its metabolites, and the growing number of identified and candidate PI kinases, suggest that many other examples of PI-modulated signaling events remain to be discovered.

Our studies described here establish that the yeast TOR2 protein is associated with the surface of the yeast vacuole and that TOR2 immunoprecipitates contain a PI-4 kinase activity. We find that the FKBP12–rapamycin complex binds wild-type TOR2 but not a TOR2 mutant that is rapamycin resistant as a result of a single amino acid substitution (S1975I). Thus TOR2, as previously predicted based on genetic findings (Heitman *et al.*, 1991a), is the direct target of the FKBP12–rapamycin complex. Surprisingly, the FKBP12–rapamycin complex does not markedly inhibit the PI-4 kinase activity associated with TOR2. Rapamycin does cause TOR2 to become delocalized from the vacuolar surface, which we propose decreases the ability of vacuolar membranes to synthesize PI4P. These studies reveal an unexpected connection between the vacuole and a rapamycin-sensitive signaling pathway regulating cell cycle progression. The similarities between rapamycin action in yeast and mammalian cells, and the recent identification of a mammalian TOR homolog (Brown *et al.*, 1994; Chiu *et al.*, 1994; Sabatini *et al.*, 1994; Sabers *et al.*, 1995), suggest that our findings should also be generally applicable to understanding immunosuppression and inhibition of cellular proliferation by FKBP12–rapamycin in multicellular eukaryotes.

Results

Identification of the TOR2 protein

To identify and characterize the TOR2 protein, and to test if TOR2 is the direct target of the FKBP12–rapamycin complex, we produced two distinct polyclonal antisera directed against TOR2. The first was raised against two peptides derived from internal amino- and carboxy-terminal regions of TOR2 that were coupled together to keyhole limpet hemocyanin (KLH) (Figure 1A). The resulting antipeptide antiserum recognizes both amino- and carboxy-terminal TOR2–trpE fusion proteins expressed in *Escherichia coli* (Figure 1B). This reaction is specific because it was not detected when total bacterial lysates were blotted with the preimmune serum or when total cell lysates of bacteria containing only the trpE fusion vector alone were blotted with the anti-TOR2 peptide antiserum (Figure 1B). More importantly, in combined immunoprecipitation Western blot experiments, the anti-TOR2 peptide antiserum, but not the preimmune serum, specifically immunoprecipitated an ~240 kDa protein from total yeast cell lysates or a yeast vacuolar fraction (see below) (Figure 1C). This 240 kDa protein is recognized in Western blot by an antiserum directed against a TOR2-C–trpE fusion protein (to be described below) (Figure 1C). These findings establish that the anti-TOR2 peptide antiserum reacts with the native TOR2 protein. Importantly, these peptides are derived from sequences unique to the TOR2 protein and are not found in other yeast proteins that share sequence identity to other regions of TOR2, including TOR1, STT4, PIK1 and ESR1/MEC1/SAD3 (Flanagan *et al.*, 1993; Garcia-Bustos *et al.*, 1994; Helliwell *et al.*, 1994; Kato and Ogawa, 1994; Yoshida *et al.*, 1994). Thus, the resulting anti-peptide antiserum is highly specific for the TOR2 protein.

An additional antiserum was raised against the carboxy-terminal region of TOR2 fused to trpE (Figure 1A). By Western analysis, both the anti-TOR2 peptide and the anti-TOR2-C–trpE antisera detected a protein present in yeast cell lysates that migrated at ~244 kDa (Figure 1D, lane 1), as calculated from semi-logarithmic plots of relative electrophoretic mobility averaged from eight different gels. TOR2 cross-reacting material increased in abundance when TOR2 was overexpressed from a 2 μ multi-copy plasmid (Figure 1D, lane 2) or from the *GAL1* promoter in a Δ*tor1* Δ*tor2* strain (Figure 1D, lane 3), and became virtually undetectable when expression from the *pGAL1-TOR2* gene in the Δ*tor1* Δ*tor2* strain was repressed by growth in glucose (Figure 1D, lane 4). When overexpressed, much of the TOR2 cross-reacting material migrated as smaller fragments, demonstrating that overexpressed TOR2 is subject to proteolytic degradation. This reaction was specific because it was not observed when

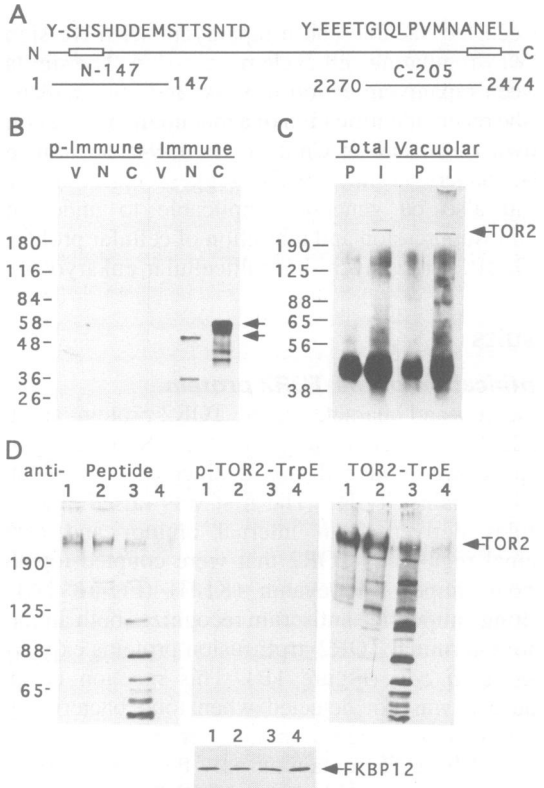

Fig. 1. Generation of antisera directed against TOR2. (**A**) Sequences of the peptides corresponding to internal amino- and carboxy-terminal TOR2 regions that were coupled together to KLH and used to generate an anti-peptide antiserum are depicted above the boxes in the linear representation of the *TOR2* gene. A TOR2–trpE fusion protein from the carboxy- (C-205) terminus was used to generate a polyclonal antiserum. Also shown in the figure is an amino-terminal TOR2–trpE fusion proteins (N-147). (**B**) The anti-peptide antiserum recognizes recombinant TOR2–trpE fusion proteins. By Western analysis, the anti-TOR2 peptide antiserum (Immune) recognizes both an amino-terminal (N-147, N) and a carboxy-terminal (C-205, C) TOR2–trpE fusion protein produced in *E.coli*. No reaction was detected with total cell lysates of bacteria transformed with the trpE fusion vector alone (V) or when these lysates were blotted with the preimmune (p-Immune) antiserum. Arrows indicate the migration position of the amino- and carboxy-terminal TOR2–trpE fusion proteins. (**C**) The anti-peptide antiserum recognizes native TOR2. Samples from the total spheroplast lysate (Total) or a vacuolar fraction (Vacuolar) of strain MLY10a (*Δtor1 TOR2*) were immunoprecipitated with the preimmune (P) serum or the anti-TOR2 peptide antiserum (I) (diluted 1:500). The immunoprecipitates were analyzed by Western blot with the anti-TOR2-C–trpE antiserum. (**D**) Western analysis with the anti-TOR2 peptide antiserum (anti-Peptide), the TOR2–trpE preimmune serum (p-TOR2-trpE) and the TOR2-C–trpE antiserum (TOR2-trpE) of equal amounts of protein extracts from yeast cells expressing *TOR2* from the chromosome (*Δtor1* strain MLY10a, lane 1), and a 2 μ plasmid-borne *TOR2* gene (*Δtor1* strain MLY10a/p2μ-TOR2, lane 2), or from a GAL promoter-driven *TOR2* gene on a *CEN* plasmid, induced with galactose (lane 3) or repressed with glucose (lane 4) in the *Δtor1 Δtor2*/pGAL1-TOR2 strain JHY89-2a. For glucose repression of TOR2 expression, strain JHY89-2a was grown to logarithmic phase in YP-galactose medium, pelleted and washed twice with 10 ml H_2O, and the cells were diluted 1:100 and grown in YP-glucose medium for 12 h at 30°C. In the lower panel, a Western blot with anti-FKBP12 antiserum demonstrates that equal amounts of protein were loaded in lanes 1, 2, 3 and 4 shown in the upper panels. The migration positions of TOR2 and FKBP12 are indicated with arrows. Numbers to the left in B, C and D indicate molecular mass in kDa.

the preimmune TOR2-C–trpE serum was employed (Figure 1D, middle panel). Taken together, these results confirm that both antisera specifically recognize the TOR2 protein.

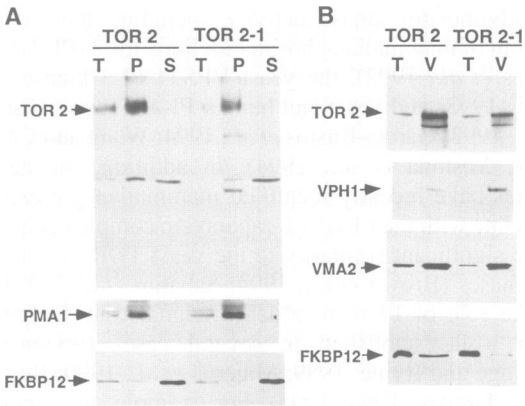

Fig. 2. TOR2 cofractionates with an insoluble vacuolar cell fraction. (**A**) Cell-free lysates of the wild-type *TOR2 Δtor1* strain MLY10a and the isogenic *TOR2-1 Δtor1* mutant strain MLY46-9c were centrifuged at 100 000 *g* and equivalent amounts of protein from the total cell lysate (T), membrane (P) and cytosolic (S) fractions were fractionated by SDS–PAGE and analyzed by Western blot with antisera directed against TOR2-C–trpE, the plasma membrane H^+-ATPase (PMA1) and the soluble protein FKBP12. (**B**) Total spheroplast lysates (T) and a vacuolar fraction (V) from the *TOR2 Δtor1* strain MLY10a, or the *TOR2-1 Δtor1* strain MLY46-9c, were analyzed by Western blot with antisera raised against TOR2 (TOR2-C–trpE), FKBP12 and the vacuolar H^+-ATPase subunits VPH1 and VMA2. Approximately 40 μg of protein were loaded in each lane.

TOR2 protein is localized to the vacuolar periphery

To localize the TOR2 protein, yeast cells expressing the wild-type TOR2 or rapamycin-resistant TOR2-1 mutant protein and deleted for the *TOR1* gene to avoid any cross-reaction were fractionated into membrane (P100) and cytoplasmic (S100) fractions. Equivalent amounts of protein from the total cell extract prior to fractionation and from the P100 and S100 fractions were analyzed by Western blot for TOR2, the plasma membrane H^+-ATPase PMA1 (Serrano, 1988) and the soluble protein FKBP12. TOR2 quantitatively cofractionated with PMA1 in the P100 fraction (Figure 2A). Only trace amounts of TOR2 were observed in the cytosolic fraction where FKBP12 was detected (Figure 2A). Thus, we conclude that TOR2 associates with an insoluble cellular fraction, suggesting that TOR2 might be membrane associated.

TOR2 was further localized by indirect immunofluorescence. A distinct ring of immunofluorescence was observed following staining with the anti-TOR2 peptide antiserum (Figure 3B). By 4′,6-diamidino-2-phenylindole (DAPI) staining of DNA, these rings are not nuclei (Figure 3A). By microscopy with Nomarski optics, these rings correspond to the surface of the vacuole (Figure 3C), which is observed as a large depression in the yeast cell.

The TOR2 vacuolar staining pattern is specific based on the following observations. First, this staining pattern was not observed with preimmune sera (Figure 3G) or when the primary antibody was omitted (data not shown). Second, the entire cytoplasm was stained when cells overexpressed TOR2 from a 2 μ plasmid (Figure 3H). Third, preadsorbing the antiserum with the TOR2-N–trpE and TOR2-C–trpE fusion proteins greatly reduced staining (Figure 3I). Fourth, a similar staining pattern, albeit with decreased intensity, was observed with the anti-TOR2-C–trpE antiserum (data not shown). Lastly, in *end1* (allelic with *vps11*) mutant cells, which lack a morphologically

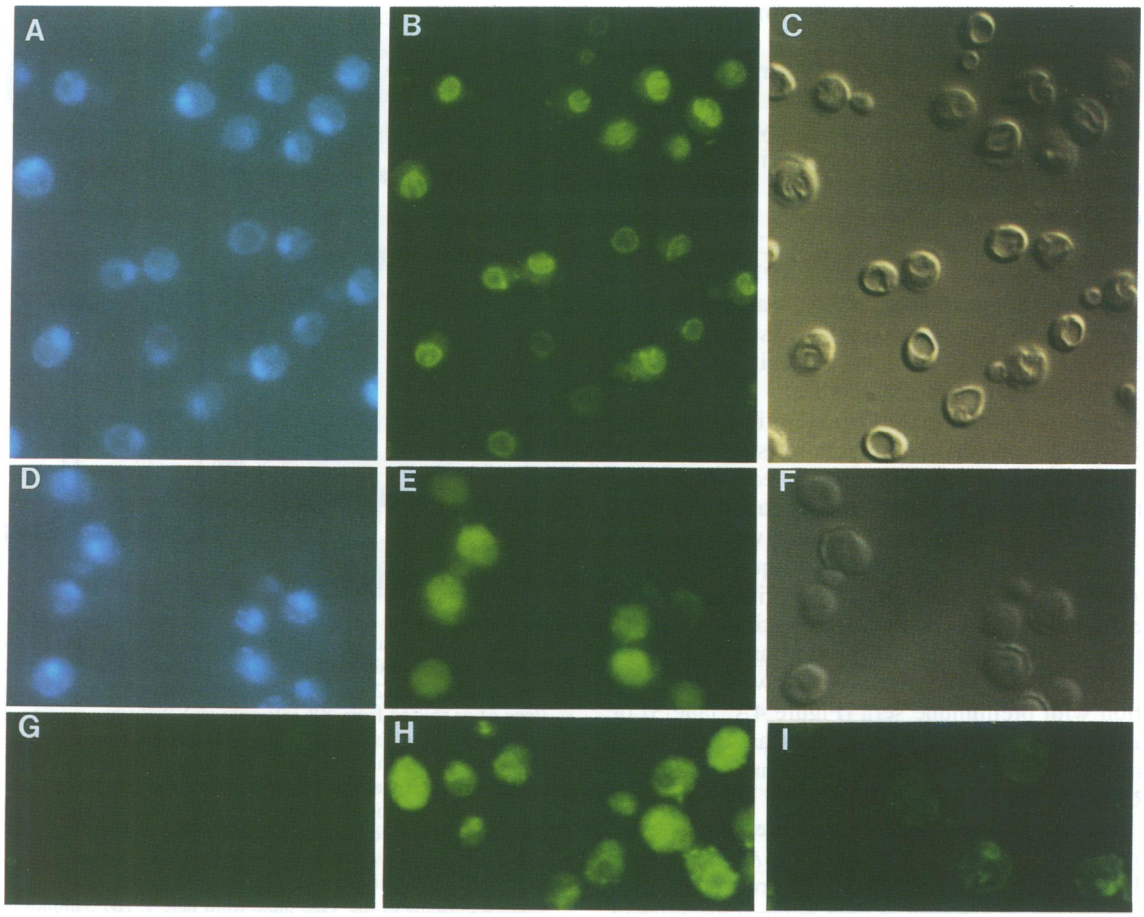

Fig. 3. TOR2 is localized to the vacuolar periphery. Cells from Δ*tor1* strain MLY10a (**A**, **B**, **C**, **G** and **I**), Δ*tor1* strain MLY10a bearing a p2μ-TOR2 plasmid (**H**) or an isogenic *end1 TOR1* mutant strain (JHY88) (**D**, **E** and **F**) were subjected to immunofluorescence as described in Materials and methods. Results presented were obtained with the preimmune serum (G) or the anti-TOR2 peptide–KLH antiserum that had been preadsorbed in whole fixed cells (B, E and H) or in whole fixed cells and nitrocellulose-immobilized amino- and carboxy-terminal TOR2–trpE fusion proteins (I). The primary antibody was detected with a fluorescein-conjugated secondary antibody and visualized with a B-2A filter set (Nikon). Nuclei were localized using DAPI and photographed through a UV-2A filter (Nikon). Cells stained with DAPI (A and D), or fluorescein (B, E, G, H and I), or visualized by differential interference contrast (Nomarski) imaging (C and F) are shown. Panels showing the same field of cells are: (A, B and C), (D, E and F).

detectable vacuole (Figure 3F), TOR2 was distributed throughout the cytoplasm (Figure 3E).

To confirm the vacuolar localization of TOR2 by an independent approach, vacuoles were isolated by Ficoll sedimentation gradients (see Materials and methods) and the total spheroplast lysate and the vacuolar fraction were analyzed by Western blot with antisera directed against the TOR2-C–trpE fusion protein, FKBP12, and the vacuolar H^+-ATPase subunits VPH1 and VMA2. TOR2 was highly enriched in the vacuolar fraction together with the vacuolar marker proteins VPH1 and VMA2 (Figure 2B), confirming that TOR2 is localized to the vacuole.

TOR2 vacuolar localization is important for TOR function

Additional data suggest that vacuolar localization is important for TOR2 function. First, both the class C Δ*end1/vps11* vacuolar mutation and a class D *vps3* vacuolar mutation confer a rapamycin-hypersensitive phenotype. The minimum inhibitory concentration (MIC) of an Δ*end1* or *vps3* mutant strain was 2.5 ng/ml compared with an MIC of 25 ng/ml for isogenic wild-type strains (data not shown). Second, a deletion mutation of the non-essential TOR2 homolog TOR1 was found to be synthetically lethal with an Δ*end1* mutation (data not shown). The observed synthetic lethality is not attributable to the slight growth defect caused by the Δ*tor1* mutation (Helliwell *et al.*, 1994), because an *fpr1* mutation, which confers an even more severe growth defect (Heitman *et al.*, 1991b), was not synthetically lethal with an Δ*end1* mutation. Thus TOR1, which is normally not essential, becomes essential when the vacuole is perturbed. Consistent with this finding, we also discovered that an Δ*end1* mutation completely prevented the *TOR2-1* mutation from conferring rapamycin resistance in a Δ*end1 TOR2-1* mutant strain. This was the case with Δ*end1 TOR2-1* double mutant strains obtained either by disrupting the *END1* gene in a *TOR2-1* mutant strain or as meiotic segregants following sporulation and dissection of a *TOR2/TOR2-1 END1/*Δ*end1* heterozygous diploid (data not shown). Thus, in the Δ*end1* mutant strain, both TOR1 and TOR2 are now essential and a TOR2-1 rapamycin-resistant mutant no longer suffices to protect the cell from rapamycin. Taken together, these findings establish that TOR2 is localized to the vacuole surface and suggest a link between vacuolar functions, TOR2 activity and FKBP12–rapamycin action.

TOR2 has an associated phosphatidylinositol-4 kinase activity

Sequence analysis of the *TOR1* and *TOR2* genes (Cafferkey *et al.*, 1993; Kunz *et al.*, 1993; Helliwell *et al.*, 1994) reveals that they share significant similarity to the mammalian 110 kDa PI-3 kinase catalytic subunit (Hiles *et al.*, 1992), the yeast PI-3 kinase VPS34 (Schu *et al.*, 1993), yeast and human PI-4 kinases (Flanagan *et al.*, 1993; Garcia-Bustos *et al.*, 1994; Wong and Cantley, 1994; Yoshida *et al.*, 1994) and mammalian FKBP12–rapamycin binding proteins (Brown *et al.*, 1994; Sabatini *et al.*, 1994). However, no enzymatic activity associated with the yeast TOR1 or TOR2 protein, or their mammalian counterpart, had as yet been characterized.

To determine whether the TOR2 protein is a PI kinase, wild-type TOR2 and the rapamycin-resistant TOR2-1 (S1975I) mutant proteins were immunoprecipitated with antiserum directed against TOR2–trpE, incubated with PI and [γ-^{32}P]ATP, and the reaction products were resolved by thin layer chromatography (TLC) and quantified with a phosphoimager (Figure 4A). Immunoprecipitated TOR2 protein exhibited readily detectable PI kinase activity (100%) (Figure 4A, lane 4). Only trace amounts of PI kinase activity (3.5%) were detected following immunoprecipitation with preimmune sera (Figure 4A, lane 3) or an unrelated antiserum directed against yeast cyclophilin A (data not shown). Preadsorption of the antiserum with the TOR2–trpE fusion proteins reduced the level of detected PI kinase activity by 70% (Figure 4A, lane 5). Finally, overexpression of TOR2 from the GAL1 promoter increased PI kinase activity by 304% (Figure 4A, lane 6), whereas repression of expression with glucose diminished activity 3-fold (Figure 4A, lane 7). In the borate TLC system, the product of TOR2 immunoprecipitates co-migrated with the [^{3}H]PI4P standard (Figure 4A, lanes 1 and 4). In addition, phosphorylation of PI by these immunoprecipitates was time dependent and was not inhibited by wortmannin, Triton X-100 or NP-40, known inhibitors of PI-3 kinases. Lastly, TOR2 immunoprecipitates did not phosphorylate PI4P (data not shown).

To establish more definitively that TOR2 immunoprecipitates produce PI4P, the product of the PI kinase reaction and [^{32}P]PI3P and [^{3}H]PI4P standards were deacylated and analyzed by high-performance liquid chromatography (HPLC) with a strong anion exchange (SAX) column. As shown in Figure 4D, the deacylated product co-migrated with the gPI4P standard.

To allay any possible concern that the anti-TOR2 antiserum is recognizing a PI-4 kinase related to TOR2, we adopted two strategies. First, having established that TOR2 is localized to the vacuole, we reasoned that TOR2-associated PI-4 kinase activity should be recovered by immunoprecipitating TOR2 from isolated vacuoles. As shown in Figure 4B, following immunoprecipitation with the anti-TOR2-C–trpE antiserum, a more highly enriched PI-4 kinase activity was recovered from isolated vacuoles compared with the total spheroplast lysate (Figure 4B, compare lanes 4 and 3). No activity was recovered in immunoprecipitations of isolated vacuoles with the preimmune serum (Figure 4B, lane 2). Thus, a TOR2-associated PI-4 kinase activity is localized to the vacuole.

As a second independent means to establish that the PI-4 kinase activity detected is not attributable to a cross-reacting related PI-4 kinase, we isolated conditional alleles of the *TOR2* gene that render TOR2 temperature sensitive (ts) for function. As described in Materials and methods, ts TOR2 mutants were obtained following *in vitro* chemical mutagenesis with hydroxylamine and a plasmid shuffle. The resulting TOR2 mutants support growth of a *Δtor2* strain at 25°C but not at 37°C. Subcloning experiments

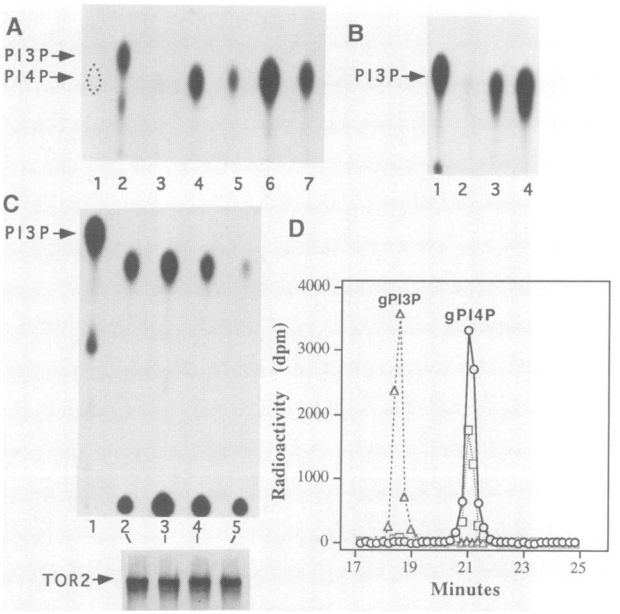

Fig. 4. TOR2 has an associated PI-4 kinase activity. (**A**) Cell extracts from the *Δtor1* strain MLY10a (lanes 3, 4 and 5) or from the *Δtor1 Δtor2/pGAL1-TOR2* strain JHY89-2a grown in YP-galactose medium (lane 6) or shifted from YP-galactose to YP-glucose medium for 10 h (lane 7) were immunoprecipitated with the preimmune serum (lane 3), the antiserum against the TOR2–trpE fusion protein (lanes 4, 6 and 7) or the antiserum that had been preadsorbed to the TOR2–trpE fusion protein (lane 5). The immunoprecipitates were analyzed for PI kinase activity as described in Materials and methods. [^{3}H]PI4P (lane 1) and [^{32}P]PI3P (lane 2) standards were included. The position of migration of the [^{3}H]PI4P standard was determined by scintillation counting of excised portions of the TLC plate from lane 1. (**B**) Samples containing 3 mg of protein of total spheroplast lysate (lane 3) or a vacuolar fraction (lanes 2 and 4) from the *Δtor1* strain MLY10a were immunoprecipitated with preimmune TOR2-C–trpE serum (lane 2) or the anti-TOR2-C–trpE antiserum (lane 3 and 4). The immunoprecipitates were assayed for PI kinase activity and analyzed by borate TLC analysis. A [^{32}P]PI3P standard was loaded in lane 1. (**C**) PI kinase assays were performed with TOR2 immunoprecipitates from 3 mg of cell extracts of wild-type TOR2 (lanes 2 and 3) and the ts TOR2 mutant *tor2-ts4* (lanes 4 and 5) isolated from cells of strain MH346-1a Δtor1 (*Δtor1 Δtor2*) expressing wild-type TOR2 or the *tor2-ts4* mutant from plasmid pML40-3 and that had been grown at the permissive (25°C, lanes 2 and 4) or the restrictive (37°C, lanes 3 and 5) temperature for 8 h prior to the analysis. The PI kinase assay was performed as described in Materials and methods except that the temperature of the assay was at 25°C (lanes 2 and 4) or 37°C (lanes 3 and 5) for 15 min. In the lower panel, the Western blot analysis with 20 μg of the cell extracts prior to immunoprecipitation with anti-TOR2 antiserum illustrates that both wild-type and the temperature-sensitive TOR2 mutant proteins are produced in the cell in roughly equal amounts at both the permissive and non-permissive temperature. (**D**) SAX HPLC analysis. Radiolabeled PI compounds were deacylated and analyzed by HPLC with a SAX column as described (Serunian *et al.*, 1991). Eluted fractions were analyzed by liquid scintillation counting. The TOR2 reaction product is indicated by circles. The elution positions of glycerophosphatidylinositol-3-phosphate (triangles, gPI3P) and glycerophosphatidylinositol-4-phosphate (squares, gPI4P), are indicated. The migration positions of PI3P and PI4P standards in A–C are indicated.

confirmed that the mutations lie within the *TOR2* gene. PI kinase activity was assayed in TOR2 immunoprecipitates from cell lysates of strain MH346-1a Δtor1 expressing wild-type TOR2 (*Δtor1 Δtor2 /TOR2*) or an isogenic *tor2* ts mutant derivative (*Δtor1 Δtor2 /tor2-ts4*) grown at the permissive (25°C) and non-permissive (37°C) temperatures. As shown in Figure 4C (lanes 2 and 4), normal levels of PI-4 kinase activity were detected from either strain grown under permissive conditions. In constrast, when grown at the restrictive temperature, PI-4 kinase activity associated with wild-type TOR2 protein was readily detected, but the PI-4 kinase activity associated with the *tor2* ts mutant protein was dramatically reduced to 11% of the activity detected with the wild-type TOR2 protein assayed under the same conditions in several independent experiments (Figure 4C, lane 5). By Western blot, both wild-type TOR2 and the ts TOR2 mutant protein were expressed at comparable levels at both 25°C and 37°C, indicating that the ts mutant protein is inactive but stably expressed at 37°C (Figure 4C, lower panel). The PI-4 kinase activity associated with the ts TOR2 mutant protein was not thermolabile *in vitro* (data not shown), which is often the case with ts mutant proteins. We note that we cannot exclude the possibility that, at the restrictive temperature, the ts mutation renders TOR2 unable to associate with a coprecipitating PI-4 kinase. We therefore conclude that the PI-4 kinase activity detected in TOR2 immunoprecipites is fully attributable to either the TOR2 protein itself or to a tightly associated PI-4 kinase. Collectively, our observations suggest that TOR2 is a subunit of a novel PI-4 kinase.

Because the yeast TOR2 protein is known to be essential for yeast viability (Kunz *et al.*, 1993), we addressed whether activity of the kinase domain of TOR2 is essential. A mutation, D2279A, was introduced into the *TOR2* gene (Materials and methods) in a region highly conserved between lipid and protein kinases, the DXHXXN loop, which the X-ray crystal structure of cAMP-dependent protein kinase reveals is involved in ATP binding and transfer of phosphate (Knighton *et al.*, 1991). A similar mutation eliminates the PI-3 kinase activity of the yeast VPS34 and renders the protein inactive (Schu *et al.*, 1993). Plasmids expressing the wild-type and the D2279A mutant *TOR2* genes were introduced into a *TOR2/Δtor2* heterozygous diploid strain. Following sporulation and tetrad dissection, wild-type *TOR2* complemented and restored viability to *Δtor2* segregants whereas the D2279A mutant *TOR2* gene did not (see Materials and methods). These findings suggest that activity of the TOR2 kinase domain is essential for viability.

FKBP12–rapamycin complex binds TOR2 but fails to bind the TOR2-1 rapamycin-resistant mutant

To test if the TOR2 protein is the target of the FKBP12–rapamycin complex, as predicted from genetic data (Heitman *et al.*, 1991a), FKBP12 affinity beads were incubated with cell extracts from wild-type TOR2 or rapamycin-resistant TOR2-1 mutant yeast strains overexpressing the corresponding TOR2 or TOR2-1 protein. Bound proteins were eluted and analyzed by Western blot with the antiserum directed against the TOR2–trpE fusion protein. With extracts from TOR2 wild-type cells, we detected binding of the TOR2 protein to FKBP12 (Figure 5, lane 2) that was stimulated ~5-fold by rapamycin (Figure 5, lane 3). TOR2 binding to the FKBP12–rapamycin complex was specific because no binding was detected with affigel in the presence of rapamycin alone (Figure 5, lane 1). Importantly, with extracts from the TOR2-1 mutant strain, no binding was detected to the FKBP12 matrix (Figure 5, lane 4) and only trace binding to the FKBP12–rapamycin complex was observed (Figure 5, lane 5). Western blot analysis confirmed that roughly equal amounts of the wild-type TOR2 and the TOR2-1 rapamycin-resistant mutant proteins were present in the extracts employed for binding assays (Figure 5, lower panel), indicating that the observed defect in binding is attributable to the single amino acid substitution in the TOR2-1 mutant protein. These results confirm that TOR2 is the relevant target of the FKBP12–rapamycin complex and reveal that the S1975I *TOR2-1* mutation confers drug resistance by preventing binding by the FKBP12–rapamycin complex.

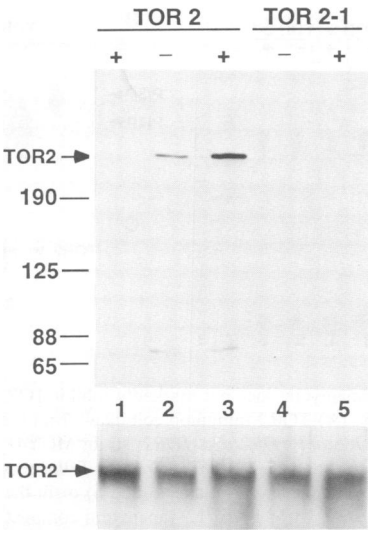

Fig. 5. Rapamycin stimulates FKBP12 binding to wild-type TOR2 but not to the rapamycin-resistant TOR2-1 mutant protein. Extracts from yeast strains lacking FKBP12 and TOR1 (to avoid competition from the endogenous proteins), and also carrying a 2 μ-based plasmid to overexpress the wild-type TOR2 protein (TOR2, strain MCY4) or the rapamycin-resistant TOR2-1 mutant protein (TOR2-1, strain MCY5), were incubated with affigel-10–FKBP12 (lanes 2 and 4) or affigel-10–FKBP12–rapamycin (lanes 3 and 5). Lane 1 is a control in which the wild-type TOR2 extracts were incubated with affigel-10 beads without FKBP12 in the presence of rapamycin. Following elution of bound material, TOR2 was detected by Western blot with the anti-TOR2-C–trpE antiserum. Values at the left indicate molecular mass in kDa. Results shown are representative of three independent experiments. The arrow shows the migration position of TOR2. (–) and (+) indicate absence and presence of rapamycin, respectively. The lower panel demonstrates by Western blot that roughly equivalent amounts of the TOR2 and TOR2-1 protein were present in the binding assays shown above.

FKBP12–rapamycin does not markedly inhibit the TOR2-associated PI-4 kinase activity

The FKBP12–rapamycin complex could inhibit TOR2 by affecting its associated PI-4 kinase activity, or by interfering with other functions, such as its ability to form complexes with effectors or to be localized properly in the cell. We therefore tested whether the FKBP12–rapamycin complex alters TOR2-associated PI-4 kinase activity *in vitro*. To avoid competition between exogenous

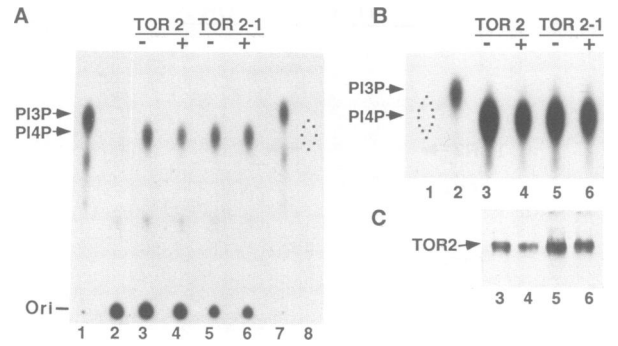

Fig. 6. FKP12–rapamycin does not markedly inhibit TOR2-associated PI kinase activity. (**A**) TOR2 immunoprecipitates from the wild-type TOR2 strain (*fpr1 Δtor1 TOR2/p2μ-TOR2*; strain MCY4) or the TOR2-1 mutant strain (*fpr1 Δtor1 TOR2-1/p2μ-TOR2-1*; strain MCY5) were incubated in the absence (–, lanes 3 and 5) or in the presence (+, lanes 4 and 6) of 1 μM FKBP12–rapamycin complex in PI kinase buffer for 15 min at 4°C. PI kinase activity in the immunoprecipitates was assayed as described in Materials and methods. The migration position of [^{32}P]PI3P (lanes 1 and 7) and [^{3}H]PI4P (lane 8, indicated by a dashed line) standards and the origin (ori) are indicated. (**B**) PI kinase activity in TOR2 immunoprecipitates from TOR2 strain JK9-3da and the TOR2-1 mutant strain R17 was assayed as in (A) except that, prior to lysis, cells in early log phase growth were incubated in the absence (–, lanes 3 and 5) or in the presence of 0.5 μg/ml rapamycin for 4 h (+, lanes 4 and 6). [^{3}H]PI4P and [^{32}P]PI3P standards were chromatographed in lanes 1 and 2, respectively. (**C**) The levels of TOR2 protein were detected by Western blot in equal amounts (corresponding to equal cell numbers) of the same cell extracts used to immunoprecipitate and assay TOR2-associated PI kinase activity in (B). Note that the decrease in PI kinase activity (45% in TOR2 and 20% in TOR2-1 strains respectively) following rapamycin treatment in (B) can be attributed to a corresponding decrease in the amount of TOR2 protein in the extract rather than to a direct inhibitory effect of FKBP12–rapamycin.

FKBP12–rapamycin and endogenous FKBP12 and TOR1, we employed cell extracts from the *fpr1 Δtor1* mutant strains in which FKBP12–rapamycin binding to TOR2 could be readily detected (Figure 5). However, when added directly to the TOR2 immunoprecipitates, the FKBP12–rapamycin complex at 1 μM exhibited only a moderate (35%) inhibition of the PI-4 kinase activity of TOR2 immunoprecipitates (Figure 6A, compare lanes 3 and 4). In comparison, the FKBP12–rapamycin complex had no effect on the PI-4 kinase activity (99% activity remained) associated with the TOR2-1 rapamycin-resistant mutant enzyme (Figure 6A, compare lanes 5 and 6).

FKBP12–rapamycin might not inhibit *in vitro* if, for example, our *in vitro* conditions fail to mimic those *in vivo*. However, when TOR2 was immunoprecipitated from wild-type yeast cells expressing FKBP12 and exposed to 0.5 μg/ml rapamycin for 4 h, we also observed only a partial apparent inhibition of TOR2-associated PI-4 kinase activity, in this case to 55% of the level detected in untreated cells analyzed in parallel (Figure 6B, lanes 3 and 4). However, when the level of TOR2 protein present in these cell extracts was assessed in parallel by Western blot, we found reproducibly that the amount of the TOR2 protein was also decreased to about the same extent in the rapamycin-treated cells (Figure 6C, lanes 3 and 4); thus, the decrease in PI kinase activity can be accounted for largely by a decrease in TOR2 protein. In experiments performed in parallel, we observed less inhibition of the PI-4 kinase activity (80% activity) associated with the TOR2-1 mutant protein by rapamycin (Figure 6B, lanes 5 and 6). In addition, the level of the TOR2-1 protein was increased ~2-fold compared with wild-type TOR2, and rapamycin had little effect on the level of the TOR2-1 mutant protein (Figure 6C, lanes 5 and 6). For both types of experiments, involving rapamycin treatment either *in vitro* or *in vivo*, we obtained results similar to those described above in at least 10 different experiments. Moreover, the extent of inhibition did not increase markedly with higher drug concentrations or longer periods of incubation (M.E.Cardenas and J.Heitman, unpublished results).

Both *in vitro* and *in vivo*, the level of inhibition of the TOR2-associated PI kinase activity by FKBP12–rapamycin would appear not to be sufficient to account for the marked toxicity of rapamycin *in vivo*. For example, diploid cells are fully viable with a single copy of the *TOR2* gene, and thus a 2-fold decrease in TOR2 activity is unlikely to be lethal. Therefore, we propose that the FKBP12–rapamycin complex does not kill the cell by directly inhibiting TOR2-associated PI-4 kinase activity. Alternatively, the FKBP12–rapamycin complex might only act on TOR2 during a specific period in the cell cycle or could inhibit TOR2 by delocalizing it away from the vacuolar surface and depriving the PI-4 kinase of its lipid substrate.

Rapamycin arrests cell cycle progression in G_1 prior to start and α-factor arrest

We first tested if TOR2-associated PI kinase activity and protein level are specifically regulated during cell cycle progression and whether they are affected by the FKBP12–rapamycin complex at a specific stage in the cell cycle. Haploid rapamycin-sensitive MATa yeast cells were synchronized in G_1 by treatment with α-factor mating pheromone. When nearly 100% synchronization was achieved, α-factor was removed and the G_1-arrested cells were then washed and transferred into medium with or without 0.5 μg/ml rapamycin. Microscopic examination revealed that the majority of the cells formed buds under both conditions. Although bud growth was ~2-fold slower compared with cells released in the absence of rapamycin, cells released into rapamycin nonetheless proceeded through the cell cycle and arrested as large, unbudded cells (Figure 7, compare panels A and D). Similar findings were observed when 0.5 μg/ml rapamycin were added 20 min prior to release from α-factor arrest (data not shown).

Analogous cell cycle arrest experiments were performed with *cdc15* and *cdc35* mutant strains to delimit the portion of the cell cycle in which FKBP12–rapamycin acts. *cdc15* and *cdc35* mutant cells were arrested in G_2–M phase or early G_1, respectively, by shift to 38°C and released into medium with or without rapamycin at 24°C. Whereas 80% of *cdc15* mutant cells released in control medium entered the cell cycle, 69% of those released into rapamycin arrested as unbudded cells. Similarly, *cdc35* mutant cells released into rapamycin remained arrested in G_1 (87–95%), whereas 83% of those released in the absence of rapamycin budded and re-entered the cell cycle. Combined with previous findings that rapamycin treatment of unsynchronized cultures induces G_1 arrest (Heitman *et al.*, 1991a), and that depletion of TOR1 and TOR2 causes

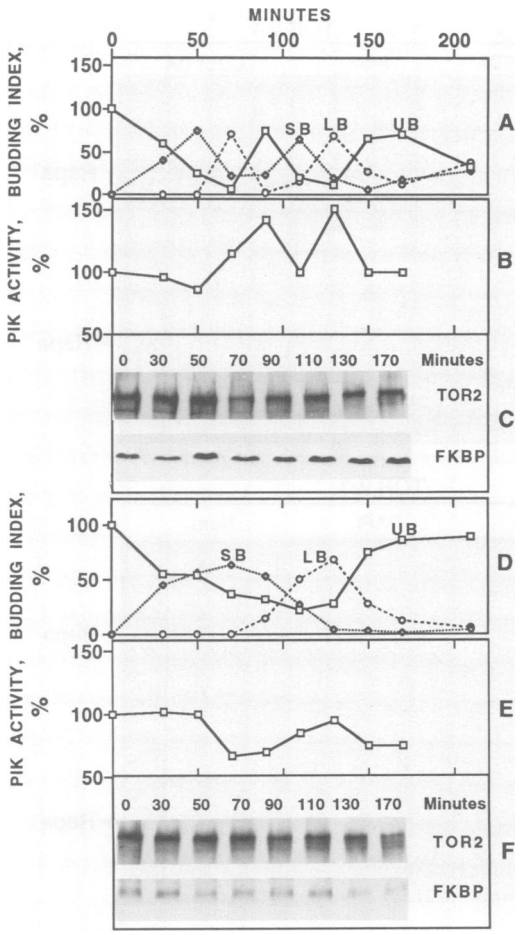

Fig. 7. Levels of TOR2 protein and TOR2 immunoprecipitated PI kinase activity do not vary significantly through the cell cycle. Cells of strain JK9-3da that had been synchronized in G_1 by α-factor treatment were released from cell cycle arrest into YPD medium (**A**, **B** and **C**) or YPD containing 0.5 μg/ml rapamycin (**D**, **E** and **F**). At 20 min intervals, aliquots of cells were removed for determination of budding index (A and D) and TOR2 PI-4 kinase activity (B and E) and detection of the TOR2 and FKBP12 proteins (C and F). For the budding index, at least 200 cells were counted with a Nikon Labophot-2 light microscope and the percentage (%) of unbudded (UB, squares), small budded (SB, diamonds) and large budded (LB, circles) cells were determined (A and D). For PI-4 kinase activity, TOR2 was immunoprecipitated from clear cell extracts prepared from equal numbers of cells. Following incubation of TOR2 immunoprecipitates with PI and [γ-^{32}P]ATP for 15 min at 26°C, products were fractionated by borate TLC. Radioactive PI4P was quantified with a phosphoimager and results shown are expressed as percentages with 100% assigned to the amount of PI4P produced with TOR2 immunoprecipitates from cells prior to release into α-factor-free medium (B and E). To determine TOR2 protein levels throughout the cell cycle, total cell extract from equal cell numbers was loaded into polyacrylamide gels and TOR2 was analyzed and detected by Western blot (C and F). The same samples were also analyzed for FKBP12 levels as a control for a protein that remains constant throughout the cell cycle. Results presented in the six panels are representative of three independent experiments.

arrest in G_1 prior to DNA synthesis (Kunz *et al.*, 1993; Helliwell *et al.*, 1994), these observations reveal that the FKBP12–rapamycin complex arrests yeast cell cycle progression in G_1 prior to start and the α-factor arrest point.

Samples of cells released from α-factor arrest in the presence and absence of rapamycin were taken at 15 min intervals, and both TOR2 protein level (Figure 7C and F) and TOR2 immunoprecipitated PI-4 kinase activity were assessed (Figure 7B and E). The TOR2 protein appears to be constant throughout the cell cycle, and this level is at most decreased by ~30% after 3 h treatment with rapamycin (Figure 7C and F). Likewise, PI-4 kinase activity associated with TOR2 did not vary significantly throughout the cell cycle. We did note that TOR2 immunoprecipitated from cells within or immediately prior to G_1 had ~50% more associated activity in comparison with other points in the cell cycle (Figure 7B). Moreover, these moderate increases in immunoprecipitated TOR2-associated PI kinase activity did not occur as cells treated with rapamycin traversed the cell cycle (Figure 7E). Based on these observations, we conclude that TOR2 protein level and associated PI-4 kinase activity, as assayed *in vitro*, are subject to only very moderate cell cycle regulation if at all. Moreover, while the FKBP12–rapamycin complex did inhibit the slight increase in TOR2-associated PI kinase activity in unbudded cells, we did not find any dramatic inhibition at a specific point in the cell cycle.

Rapamycin treatment or depletion of TOR1 and TOR2 causes cells to develop large vacuoles

To assess vacuolar localization of TOR2 further, and also the contribution of TOR2 to vacuolar function and correspondingly the role of the vacuole in TOR2 function, we monitored vacuolar morphology following depletion or inhibition of TOR protein function. When expression from a *pGAL-TOR2* gene in a *Δtor2* host strain was repressed by shifting to glucose medium, cells arrested randomly in the cell cycle (Figure 8A), as previously reported (Kunz *et al.*, 1993). Both the cell and the vacuole were somewhat enlarged in TOR2-depleted cells compared with those expressing TOR2 (Figure 8A).

In contrast, when TOR2 was depleted by repression of the *pGAL-TOR2* gene in a *Δtor1 Δtor2* mutant strain, the cells arrested uniformly as large unbudded cells (Figure 8A), as described previously (Kunz *et al.*, 1993). Remarkably, the vacuole becomes extremely enlarged in cells depleted of both TOR1 and TOR2 (Figure 8A). In such cells, the vacuole encompasses virtually the entire cell, as viewed by Nomarski optics. By DAPI staining, the nucleus in such cells becomes compressed into the small amount of remaining space (data not shown). This phenotype of vacuolar enlargement is not specific for cells depleted of TOR function, and has been observed previously for class D vacuolar protein sorting mutants, which include mutations such as *vps3* and *vps34* (Raymond *et al.*, 1990, 1992). Furthermore, large vacuoles are formed when yeast cells are starved for glucose or suffer perturbations of the actin cytoskeleton (Novick *et al.*, 1989; Pringle *et al.*, 1989). Therefore, the lethal effects of the FKBP12–rapamycin complex are unlikely to be attributable to cell death secondary to an enlarged vacuole.

Vacuolar morphology was also assessed in cells treated with rapamycin (Figure 8B). As is the case in cells depleted of TOR1 and TOR2, wild-type cells treated with rapamycin arrested in the cell cycle as unbudded cells and developed extremely large, round vacuoles, whereas TOR2-1 rapamycin-resistant mutant cells treated with rapamycin did not arrest and their vacuolar morphology was unaltered (Figure 8B). When cells were stained with the vital dye CDCFDA, which diffuses into the cell and

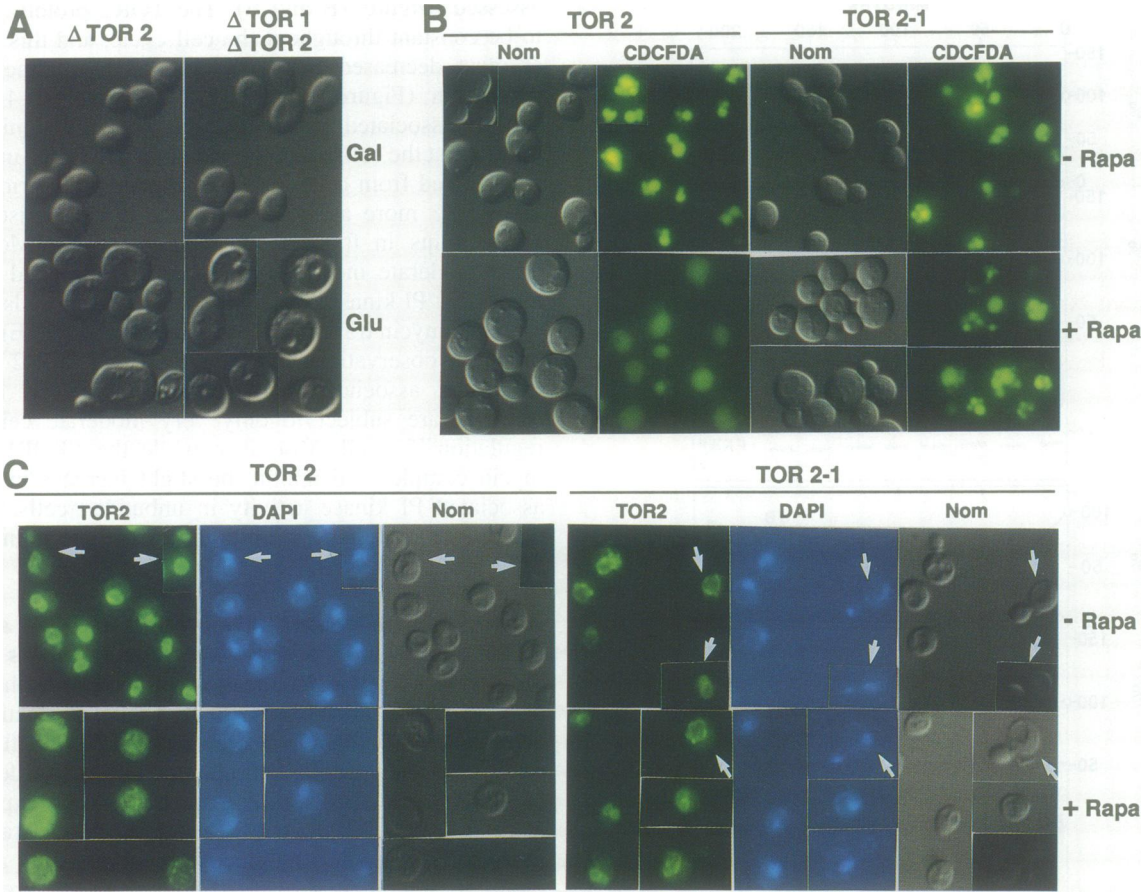

Fig. 8. Rapamycin causes cellular delocalization of TOR2 and perturbs vacuolar morphology. (**A**) Depletion of both TOR1 and TOR2 results in a large vacuolar phenotype. Strains with genotype *Δtor2/pGAL-TOR2* (strain MH343-30b) and *Δtor1 Δtor2/pGAL-TOR2* (JHY89-2a) were grown to mid-log phase in YP medium containing 2% galactose (Gal). Cultures were washed twice with YP medium containing 2% glucose (Glu), and then diluted into YP-galactose and YP-glucose media to express and repress TOR2 expression, respectively. After incubation for 12 h at 30°C with gentle shaking, portions of each culture were viewed by Nomarski optics. (**B**) Rapamycin treatment causes a large vacuole phenotype in wild-type TOR2 cells but not in TOR2-1 rapamycin-resistant cells. Cultures of wild-type TOR2 (strain JK9-3da) or TOR2-1 rapamycin-resistant cells (strain JHY12-9d) were grown to OD_{600} = 0.5. The cultures were divided and each half was treated without (–Rapa) or with 0.5 μg/ml rapamycin (+Rapa), respectively, for 3 h at 30°C. Vacuoles were stained with the vital stain CDCFDA and photographed with Nomarski optics (Nom) or by epifluorescence (CDCFDA) through a B-2A FITC filter set (Nikon). (**C**) Rapamycin causes cellular delocalization of TOR2 and the TOR2-1 mutation delays the timing of vacuolar segregation. Rapamycin-treated (+Rapa) or untreated (–Rapa) cultures of TOR2 wild-type (strain JK9-3da) or rapamycin-resistant TOR2-1 mutant (strain JHY12-9d) cells, prepared as described in (B), were processed for TOR2 immunofluorescence (see Materials and methods). The TOR2 immunofluorescence signal and nuclei stained with DAPI were photographed as indicated in the legend to Figure 3. Vacuolar morphology was observed by Nomarski optics (Nom). Arrows in fields of TOR2 wild-type cells show two budded cells in which vacuolar segregation has preceded nuclear segregation, as expected for wild-type cells. Arrows in fields of TOR2-1 cells show three budded cells in which vacuolar segregation has been delayed such that the nucleus has migrated into the buds first. Note that this unusual order of organelle segregation is not affected by rapamycin treatment (see budded cell indicated by arrow in the TOR2-1 +Rapa panel). We note that some of the fields presented in Figure 8 are composite images.

fluoresces in the acidic conditions of the yeast vacuole, we observed that the vacuole in wild-type cells was actually comprised of multiple, interconnected compartments (Figure 8B, CDCFDA), as has been observed previously (Raymond *et al.*, 1992). Following treatment with rapamycin, these multiple vacuolar compartments appeared to coalesce into a single, large, round vacuole that was poorly acidified, as evidenced by decreased and rapid quenching of CDCFDA fluorescence (Figure 8B). Remarkably, rapamycin did not alter vacuolar morphology or acidification in TOR2-1 rapamycin-resistant cells (Figure 8B).

Because a variety of conditions can affect yeast vacuolar morphology (Pringle *et al.*, 1989), we sought to exclude that this was attributable to a non-specific effect resulting from G_1 cell cycle arrest. Cultures of a *cdc28* mutant strain were grown at 22°C or temperature shifted to 37°C for 4 h prior to staining with CDCFDA. Temperature shift imposed a late G_1 arrest as large unbudded cells in ~90% of *cdc28* mutant cells. Under both conditions, the vacuole was not enlarged and remained as multiple, interconnected compartments with no acidification defect, as assessed by CDCFDA staining (data not shown). Thus, the effects of rapamycin on vacuolar morphology cannot be solely attributable to a non-specific effect of G_1 arrest.

During the course of these studies, we made the surprising observation that segregation of the vacuole during cell cycle progression was influenced by the TOR2 protein. As observed previously (Raymond *et al.*, 1990), we found that, in wild-type cells, vacuole segregation invariably preceded nuclear segregation. Thus, we observed buds with a vacuole but no nucleus, but no buds

with a nucleus and no vacuole (Figure 8C, TOR2, arrows). Moreover, all buds with a nucleus also had a vacuole. In contrast, in the isogenic TOR2-1 mutant strain, the order of vacuolar and nuclear segregation was invariably reversed. In this case, budded cells were observed with a nucleus in the bud but no vacuole, and no buds were observed with a vacuole but no nucleus (Figure 8C, TOR2-1, arrows). The TOR2-1 mutation most likely only delays vacuolar segregation, because we did not observe an increased number of cells lacking a vacuole, as one might have expected if the TOR2-1 mutation completely prevented vacuolar segregation. However, our results do not rule out the possibility that the vacuoles observed in the TOR2-1 daughter cells have arisen by *de novo* synthesis, which has been proposed previously as possibly occurring in the case of the *vps3* mutant (Raymond *et al.*, 1990). Taken together, these observations reveal that TOR function is required for the maintenance of normal vacuolar morphology and acidification, and also for proper vacuolar segregation during cell cycle progression.

FKBP12–rapamycin delocalizes TOR2 from the vacuolar periphery

Our observations suggest that TOR2 function is intimately related to its vacuolar localization. Therefore, we tested whether treatment of cells with rapamycin has any effect on TOR2 intracellular localization. To assess the effects of rapamycin on intracellular localization of TOR2, we performed indirect immunofluorescence with the anti-TOR2 peptide antisera. In this case, it proved necessary to employ gentler immunostaining conditions because cells treated with rapamycin are less sturdy and adhered more poorly compared with wild-type cells. We therefore adopted a procedure (Pringle *et al.*, 1989) in which cells are fixed with paraformaldehyde at 25°C for 2 h and then overnight at 4°C, and the acetone/methanol permeabilization step and detergents from all the buffers (employed for the experiment shown in Figure 3) are omitted. By these modifications, we were able to retain normal cellular morphology, as assessed by Nomarski optics, in rapamycin-treated cells (Figure 8C).

With this alternative immunofluorescence procedure, as described above (Figure 3), the anti-TOR2 antiserum yields a ring staining pattern that, by Nomarski, corresponds to the surface of the vacuole (Figure 8C). In marked contrast, in the vast majority of wild-type cells treated with 0.5 μg/ml rapamycin, TOR2 staining was no longer localized to discrete ring structures but was instead diffuse and largely distributed throughout the cell (Figure 8C). This perturbation in TOR2 localization by rapamycin is specific based on the following observations. First, despite enlargement and rounding, the vacuoles remained intact, as viewed by Nomarski optics, in the majority of rapamycin-treated cells. A peripheral vacuolar localization of TOR2 was also observed in an isogenic *vps3* deletion strain, which exhibits a large vacuole phenotype (data not shown). Thus, the perturbation in TOR2 localization by rapamycin is not attributable to a non-specific effect resulting from gross disruptions in vacuolar integrity or morphology. Second, the anti-TOR2 antiserum decorated distinct vacuolar ring structures in TOR2-1 mutant cells cultured in either the absence or the presence of rapamycin (Figure 8C). Thus, the TOR2-1 mutation confers rapamycin resistance and also prevents the rapamycin-dependent perturbation of TOR2 localization observed in wild-type TOR2 cells. These observations suggest that the FKBP12–rapamycin complex may inhibit TOR2 function *in vivo* by delocalizing the protein and depriving the TOR2-associated PI-4 kinase activity of its *in vivo* substrate: PI in the vacuolar membrane.

Discussion

The immunosuppressants CsA, FK506 and rapamycin have proven valuable reagents to define the molecular mechanisms of signal transduction (Schreiber, 1991; Heitman *et al.*, 1992; Schreiber and Crabtree, 1992; Liu, 1993; Cardenas *et al.*, 1994a). The target of the CsA–cyclophilin A and FKBP12–FK506 immunophilin–drug complexes has been identified as calcineurin (J.Liu *et al.*, 1991, 1992), a protein phosphatase that plays a central role in transducing signals from the activated T-cell receptor to transcription factors required for T-cell activation (Clipstone and Crabtree, 1992; O'Keefe *et al.*, 1992). In contrast, the target of rapamycin, which inhibits the interleukin-2 signaling cascade, has proven more elusive.

Biochemical studies and yeast genetics established that, like FK506, rapamycin acts by first binding FKBP12 (Bierer *et al.*, 1990; Dumont *et al.*, 1990a; Heitman *et al.*, 1991a). The isolation of rapamycin-resistant yeast mutants first identified the *TOR1* and *TOR2* genes, and the observation of non-allelic non-complementation between certain FKBP12, TOR1 and TOR2 mutations led to the proposal that the TOR proteins would be the direct targets of the FKBP12–rapamycin complex (Heitman *et al.*, 1991a). The recent identification of a mammalian TOR homolog that physically associates with the FKBP12–rapamycin complex further supports this prediction (Brown *et al.*, 1994; Chiu *et al.*, 1994; Sabatini *et al.*, 1994; Sabers *et al.*, 1995).

In the studies described here, we have employed specific antisera to detect, characterize and immunolocalize the TOR2 protein. In total cell extracts, TOR2 can be detected as an ~244 kDa protein. Surprisingly, by indirect immunofluorescence, cellular fractionation and immunoprecipitation of TOR2 PI-4 kinase activity, we find that TOR2 is localized to the surface of the yeast vacuole (Figures 2, 3 and 4B), and several observations suggest that vacuolar localization is significant for TOR2 function. We demonstrate for the first time that immunoprecipitated TOR2 exhibits readily detectable PI-4 kinase activity (Figure 4). The PI-4 kinase activity in TOR2 immunoprecipitates is temperature sensitive when obtained from a TOR2 temperature-sensitive conditional mutant grown at 37°C (Figure 4C), and is recovered from vacuolar fractions (Figure 4B). Thus, the TOR2-associated PI-4 kinase activity could be intrinsic to the TOR2 protein itself, which would be consistent with the sequence identity TOR2 shares with other known PI-4 and PI-3 kinases. Alternatively, the TOR2-associated PI-4 kinase activity could be attributable to a distinct protein that tightly associates with and coimmunoprecipitates with TOR2. For example, the TOR2 ts mutation might affect the ability of TOR2 to physically associate with a lipid kinase. Further study will be required to resolve this issue.

We demonstrate here that wild-type TOR2 binds to an FKBP12–rapamycin affinity matrix, whereas a rapamycin-

resistant TOR2-1 mutant protein does not (Figure 5). We found little inhibition of immunoprecipitated TOR2-associated PI-4 kinase activity by FKBP12–rapamycin, either *in vivo* or *in vitro* (Figure 6); however, rapamycin did lead to a delocalization of TOR2 from the vacuole (Figure 8) and preliminary *in vivo* labeling studies to examine synthesis of phospholipids in vacuolar membranes reveal that rapamycin decreases vacuolar PI4P synthesis (M.C. and J.Heitman, unpublished results). These observations demonstrate that TOR2 is one of the direct targets of the FKBP12–rapamycin complex and suggest that rapamycin may inhibit TOR2 function by perturbing intracellular localization and thereby depriving the TOR2-associated PI-4 kinase activity of its *in vivo* substrate: PI in vacuolar membranes.

Two different PI-4 kinases have been identified previously in yeast: PIK1 (Flanagan *et al.*, 1993; Garcia-Bustos *et al.*, 1994) and STT4 (Yoshida *et al.*, 1994). In addition, two membrane-associated proteins of 45 and 55 kDa with PI-4 kinase activity have been identified in yeast (Nickels and Carman, 1993), and could be encoded by additional genes. How these multiple yeast PI-4 kinases produce the same product yet direct their activities to different functions, at least one of which is essential (PIK1), is likely to involve differences in cellular localization, cell cycle regulation or interactions with proteins that metabolize or respond to PI4P. For example, the STT4 PI-4 kinase is a component of the yeast phosphokinase C pathway (Yoshida *et al.*, 1994) regulating cell wall synthesis. The PIK1 PI-4 kinase (Flanagan *et al.*, 1993) has been shown recently to be nuclear associated (Garcia-Bustos *et al.*, 1994). Previously, the yeast VPS34 protein was identified as a PI-3 kinase required for vacuolar protein sorting (Schu *et al.*, 1993). Our findings that TOR2 is vacuolar and has an associated PI-4 kinase activity reveal a second link between vacuolar function and PI metabolism.

Recent studies have identified a yeast protein, FAB1, which could participate with TOR2 in regulating vacuolar morphology and acidification (Yamamoto *et al.*, 1995). FAB1 shares sequence identity with another class of lipid kinase recently characterized from mammalian cells, phosphatidylinositol-4-phosphate 5-kinase or PI-5 kinase, which phosphorylates PI4P to generate $PI4,5P_2$ (Boronenkov and Anderson, 1995). Intriguingly, yeast mutants lacking FAB1 are viable but have large, poorly acidified vacuoles (Yamamoto *et al.*, 1995), similar to yeast cells treated with rapamycin or depleted of the TOR proteins. Although the intracellular localization and enzymatic activity of FAB1 are not yet known, these findings suggest TOR2-associated PI-4 kinase and FAB1 may cooperate to synthesize $PI4,5P_2$ in vacuolar membranes, and that this lipid product could be involved in vacuolar morphology and function. Two distinctions are that TOR2 is essential whereas FAB1 is not, and secondly that TOR2 is required for cell cycle progression whereas FAB1 is not. One possibility is that the PI-5 kinase is redundant whereas the TOR2-associated PI-4 kinase is not. Alternatively, PI4P may substitute for $PI4,5P_2$ when FAB1 is absent. Lastly, TOR2 may serve two roles in the cell: first, in cooperation with FAB1, to regulate $PI4,5P_2$ production and vacuolar functions, and second, a unique role to regulate cell cycle progression.

Why might a TOR2-associated vacuolar PI-4 kinase activity be involved in regulating cell cycle progression? The vacuole has not been thought previously to be involved in cell cycle regulation. Functions that have been ascribed to the vacuole include: creation of an acidic environment in which degradation of proteins and destruction of endocytosed material occurs, sequestration of ions, such as calcium and zinc and, importantly, storage of metabolites and nutrients, including phosphate and amino acids (Klionsky *et al.*, 1990). It is noteworthy that, aside from the plasma membrane, the largest membrane surface in yeast cells is the vacuolar membrane. Moreover, because PI-4 kinases probably act on lipids in the context of a membrane, the vacuolar surface provides a large, dispersed surface upon which to generate a lipid second messenger. Thus, the vacuole is well positioned to sense the metabolic state of the cell and to communicate this information to downstream effectors. For example, one plausible role for TOR2 is to trigger cell cycle progression by regulating PI4P production in response to appropriate levels of nutrients. In fact, the point at which FKBP12–rapamycin arrests the yeast cell cycle, in late G_1 just prior to start, has been associated previously with arrest of the cell cycle by nutrient deprivation in yeast.

It had been established previously that inositol is an essential nutrient in yeast (Becker and Lester, 1977). Furthermore, one would expect that if the PI4P produced by the TOR2-associated lipid kinase activity is required, synthesis of the precursor PI should also be essential. In fact, deletion of the gene encoding PI synthase is lethal in yeast (Nikawa *et al.*, 1987). PI synthase is largely localized in the yeast endoplasmic reticulum (ER), which is thought to be the predominant site of PI synthesis (Paltauf *et al.*, 1992). PI is likely to be transported from the ER to other organelles, such as the Golgi and vacuole, by vesicle traffic. Interestingly, a PI transfer protein localized in the Golgi (PITP/SEC14) is required for viability in yeast (Aitken *et al.*, 1990; Bankaitis *et al.*, 1990). One critical function of SEC14 might be to transfer PI from its site of synthesis to supply substrate to the TOR2-associated PI-4 kinase in the vacuole. In summary, all of these observations are consistant with TOR2 providing a vital function in yeast by regulating a novel PI-4 kinase activity in the vacuolar membrane. This view is also consistent with what is known about PI metabolism and signaling in response to nutrients in yeast. For example, introduction of a $PI4,5P_2$-specific monoclonal antibody by electroporation is lethal to yeast cells, suggesting that $PI4,5P_2$ serves an essential function (Uno *et al.*, 1988). Following glucose addition to glucose-starved yeast cells, PI4P and $PI4,5P_2$ are not cleaved by PLC (Hawkins *et al.*, 1993). Instead, under these conditions, yeast cells produce large amounts of glyceroPI4P and glyceroPI4,5P_2, which are water-soluble metabolites produced by the action of a phospholipase B or the combined action of phospholipases type A1 and A2 (Hawkins *et al.*, 1993). However, the responsible phospholipases, their regulation by carbon source and the role of such metabolites, if any, have as yet not been identified. Conversely, following addition of a nitrogen source to nitrogen-starved yeast cells, an increase in $I1,4,5P_3$ production has been observed, suggesting that a PLC may be operating under these conditions (Schomerus and Kuntzel,

1992). Finally, addition of ergosterol to sterol-depleted yeast cells leads to a moderate increase in the rate of PIP and PIP_2 synthesis (Dahl and Dahl, 1985; Dahl *et al.*, 1987). Thus, under a variety of conditions in which different classes of nutrients are added to starved yeast cells, the cumulative evidence suggests that signal transduction events mediated by PI4P metabolites might be operative. Further study will be required to test TOR2 participation in such events.

We have presented evidence that inhibition or depletion of TOR2 alters vacuolar morphology and acidification, and, moreover, that the TOR2-1 mutation delays vacuolar segregation (Figure 8). What might be the role(s) of the TOR2-associated PI-4 kinase in vacuolar functions, morphology and segregation? PI4P and $PI4,5P_2$ are known to bind proteins associated with the cytoskeleton, such as profilin and gelsolin (Janmey and Stossel, 1987; Goldschmidt-Clermont *et al.*, 1990). Thus, a possible role for the TOR2-associated PI-4 kinase may be to generate phospholipids that act as points of attachment that anchor the vacuolar membrane to the cytoskeleton. Such attachments might promote directed transport of vesicles destined to or from the vacuole and the Golgi, the plasma membrane or endosomes. It is tempting to speculate that these attachment points are subject to dynamic change due to the polarized growth experienced by the actin cytoskeleton, and that it is this polarization that mediates vacuolar segregation from mother to daughter cells. In this context, the TOR2-1 mutation may perturb the ability of the vacuole to sense actin polarization. An alternative means by which TOR2 regulation of PI4P production might alter vacuolar functions is the hypothesis that generation of acidic phospholipids, such as PI4P, in a restricted portion of a membrane might promote membrane surface protrusions as a result of membrane remodeling secondary to the electrostatic repulsion of neighboring acidic lipids (Sheetz and Singer, 1974). In this case, TOR2 action might promote the formation of structures which permit vacuole segregation into the buds of dividing cells (Weisman and Wickner, 1988).

We would like to summarize our findings in a model (Figure 9) which envisages TOR2 as a sensor for energy (ATP) and nutrient (carbon, nitrogen, phosphorus, lipid) availability. In the presence of these required nutrients, TOR2-associated PI-4 kinase activity synthesizes PI4P in the vacuolar membrane and PI4P, or a metabolite, signals to the cell cycle machinery to pass start and enter the cell cycle. In addition, the presence of PI4P or further metabolites in the vacuolar membrane provides attachment points for the vacuole to the polarized actin cytoskeleton to facilitate proper vacuolar morphology and segregation. In the presence of the FKBP12–rapamycin complex, TOR2 is bound by the protein–drug complex, resulting in the delocalization of TOR2 from the vacuolar membrane. Thus, the TOR2-associated PI-4 kinase would be unable to utilize PI in this membrane, resulting in decreased vacuolar PI4P synthesis. This results in a profound perturbation of vacuolar morphology and extinguishes the signal (PI4P) that would have started the cell cycle appropriately in response to nutrient availability. Further studies will be required to define the upstream events that regulate TOR2 activity or localization, and the downstream effectors of PI4P.

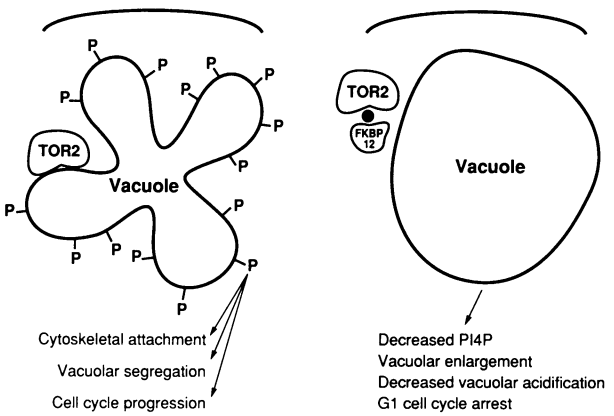

Fig. 9. Model for the role of TOR2 and PI4P in vacuolar function, cell cycle progression, and rapamycin action. In wild-type cells (left figure), the TOR2-associated PI-4 kinase activity is localized to the surface of the yeast vacuole and generates PI4P in the vacuolar membrane which, we propose, serves as the point of attachment between the vacuolar membrane and PI binding proteins associated with the actin cytoskeleton. Such attachments may give rise to the normal vacuolar architecture observed in wild-type cells, consisting of multiple interconnected structures. Because vacuolar segregation precedes nuclear segregation in wild-type TOR2 cells whereas the order of segregation is reversed in TOR2-1 mutant cells, we propose that TOR2, and possibly also PI4P, normally participates in vacuolar segregation. Lastly, because depletion or rapamycin inhibition of TOR2 and TOR1 causes cell cycle arrest, we propose that PI4P promotes cell cycle progression. In rapamycin-treated cells (right figure), the FKBP12–rapamycin complex binds TOR2, causing TOR2 to delocalize from the vacuolar surface. This results in a defect in PI4P synthesis in the vacuolar membrane, vacuole detachment from the actin cytoskeleton, the development of large, round, poorly acidified vacuoles and arrest in the G_1 phase of the cell cycle.

Materials and methods

Yeast strains and plasmids

Saccharomyces cerevisiae strains used in all experiments, except the cdc cell cycle arrests, were JK9-3D **a**/α, **a**, or α *ura3-52 leu2-3,112 trp1-1 his4 rme1 HMLa* (Heitman *et al.*, 1991a,b) or isogenic derivatives (with only changes indicated): R17, *MAT*α *TOR2-1 HIS*$^+$; MLY10α, *MAT*α *tor1Δ::LEU2 TRP*$^+$; MLY10a, *MAT***a** *tor1Δ::LEU2 TRP*$^+$; MLY46-9c, *MAT***a** *Δtor1::LEU2 TOR2-1*; MH343, *MAT***a**/α *TOR2/Δtor2::LEU2*; MH343-30b, *MAT***a** *Δtor2::LEU2* (pGAL1-TOR2); MH346–1a, *Δtor2::ADE2* (p2μ-TOR2); JHY89-2a, *MAT***a** *tor1Δ::LEU2 tor2Δ::LEU2* (pGAL1-TOR2); JHY88, *MAT***a** *end1Δ::LEU2*; JHY78, *MAT*α *TOR2-1 end1Δ::LEU2*; MCY4, *MAT***a** *tor1Δ::LEU2 fpr1::ADE2-2 TRP1 Δade2* (p2μ-TOR2); MCY5, *MAT***a** *tor1Δ::LEU2 fpr1::ADE2-2 TOR2-1* (p2μ-TOR2-1); JHY12-9d, *MAT***a** *HIS*$^+$ *TOR2-1*; JHY92, *MAT***a**/α *END1/end1Δ::LEU2 TRP1/trp1*; JHY95, *MAT***a**/α *TOR2-1/TOR2 END1/end1Δ::LEU2 HIS4/his4*; JHY96, *MAT***a** *vps3Δ1::LEU2*. cdc mutants used for cell cycle arrest studies were strains: HR178-2b, *MAT***a** *leu2 his4 ura3 bar1 cdc35*; 427, *MAT***a** *ade2 his3 leu2 trp1 ura3 bar1::URA3 cdc15-2*.

Plasmids p2μ-TOR2, pTOR2-D2279A (described below) and pTOR2-1 bear the *TOR2* gene or mutant derivatives on the 2 μ *URA3* plasmid pSEY18. Plasmid pGAL1-TOR2 expresses *TOR2* from the *GAL1* promoter of plasmid pSEY68 (Kunz *et al.*, 1993). The *TOR2-1* rapamycin-resistant allele (Heitman *et al.*, 1991a) was retrieved from the genome by repair of a *Bgl*II-gapped *TOR2* gene introduced into *TOR2-1* strain R17, and identified as a S1975I substitution (AGT→AGG mutation) by sequence analysis with primer 5′-GAATTTTGGAACG-ATATTTCCCTCAAAG. The *END1/VPS11* gene was disrupted/deleted by transformation with pVD7-D2 plasmid DNA cleaved with *Hin*dIII and *Sph*I, selection for growth on synthetic medium lacking leucine, and appearance of known phenotypes, as described (Dulic and Riezman, 1989). The *VPS3* gene was deleted by transformation with *Bam*HI-cleaved pCKR70A plasmid DNA, selection for growth in the absence of leucine and identification of transformants with the known *vps3* mutant phenotype (large vacuoles) (Raymond *et al.*, 1990).

PCR overlap mutagenesis; assay of TOR2 D2279A function

The *TOR2* D2279A mutation was generated by PCR overlap mutagenesis (Ho *et al.*, 1989) of the cloned wild-type *TOR2* gene with mutagenic primers (5′-GGGGTTAGGTG**CT**CGCCACCCTAGTAATTTG and 5′-CAAATTACTAGGGTGGCG**AG**CACCTAACCCC) and flanking primers spanning *Sal*I sites (5′-GTTTTG**GTCGAC**CAGGCTGAA-CTTGTCAGCCACG and 5′-GCCAAGCTTGCATGCCTGCAG**GTCG-AC**TCTAGAGG). The resulting 3000 bp PCR product was cleaved with *Sal*I, used to replace the fragment of the WT *TOR2* gene in pTOR2, and confirmed by DNA sequence analysis.

Plasmids expressing wild-type or D2279A mutant TOR2 protein were introduced into the *TOR2/Δtor2::LEU2* heterozygous diploid strain MH343, sporulated, and meiotic segregants isolated by micromanipulation. The parental *TOR2/Δtor2::LEU2* strain yielded 14 two viable:two inviable, and one one viable:three inviable tetrads, and all viable segregants were leu$^-$, in agreement with a previous report that TOR2 is essential (Kunz *et al.*, 1993). In contrast, whereas expression of wild-type *TOR2* rescued *Δtor2* segregants, *TOR2/Δtor2 (pTOR2)* strain yielded six two viable leu$^-$:two viable Leu$^+$ Ura$^+$ and 10 two viable leu$^-$:two inviable tetrads, the D2279A mutant TOR2 did not rescue *Δtor2* [*TOR2/Δtor2 (pTOR2-D2279A)*] and yielded 15 two viable leu$^-$:two inviable and one one viable leu$^-$:three inviable tetrads.

Generation of anti-TOR2 and FKBP12 polyclonal antisera

Portions of the *TOR2* gene encoding amino- (1–147) and carboxy-terminal (2270–2474) fragments were PCR amplified (amino-terminal oligos: 5′-GCCCGGATCCAATGAATAAATACATTAACAAATACACC and 5′-GCACCTGCAGCTACTTCTCACTTGAAGTAAACCCG; carboxy-terminal oligos: 5′-GCCCGGATCCAATGACCGGTTATATATT-GGGG and 5′-GCACCTGCAGCTACCAGAATGGACACCAACCG), cleaved with *Bam*HI–*Pst*I and cloned in the trpE fusion vector pATH22 (Koerner *et al.*, 1991). The resulting TOR2-N–trpE and TOR2-C–trpE fusion proteins were overexpressed as described (Koerner *et al.*, 1991). The TOR2-C–trpE fusion protein was gel purified, electroeluted and used to immunize rabbits according to standard procedures (Harlow and Lane, 1988). A single rabbit polyclonal antiserum was also generated against two TOR2 synthetic peptides that were coupled together to KLH (Figure 1A).

The anti-FKBP12 polyclonal antiserum was produced by injecting a rabbit with the yeast His6–FKBP12 recombinant protein obtained as described in Cardenas *et al.* (1994b). By Western analysis, the resulting antiserum recognizes a 12 kDa protein expressed by *FPR1* yeast strains but not by isogenic *fpr1* mutants lacking FKBP12 (M.E.Cardenas and J.Heitman, unpublished results). By indirect immunofluorescence analysis, this antiserum stains both the cytosol and the nucleus but is excluded from the vacuolar lumen.

The anti-PMA1 antiserum was generated and characterized as previously described (Cardenas *et al.*, 1990). Monoclonal antibodies against the vacuolar ATPase subunits VPH1 and VMA2 were purchased from Molecular Probes and kindly provided by Morris Manolson, respectively.

Cellular fractionation

Cells from the wild-type *TOR2 Δtor1* strain (MLY10a) and the *TOR2-1 Δtor1* mutant strain (MLY46-9c) were disrupted with glass beads in lysis buffer [20 mM Tris–HCl pH 7.5, 100 mM KCl, 0.1 mM EDTA, 100 μM Na_3VO, 25 mM β-glycerophosphate, 25 mM NaF, 1 μg/ml pepstatin, 1 mM benzamidine, 100 U/ml trasylol and 0.5 mM phenylmethylsulfonyl fluoride (PMSF)], and the cell lysate was spun at 1000 *g* for 5 min to remove unbroken cells. The cell-free lysate was centrifuged at 100 000 *g* for 30 min to yield membrane (P) and cytosolic (S) fractions. For Western blot analysis, aliquots containing equivalent amounts of protein from the total cell lysates and the P100 and S100 fractions were loaded for SDS–PAGE. Western blot with rabbit antisera directed against the TOR2-C–trpE fusion protein and the plasma membrane H^+-ATPase (PMA1) were performed as indicated below.

Lipid kinase assays

For lipid kinase reactions, cell pellets from 100 OD_{600} units were disrupted with glass beads in 0.5 ml of lysis buffer (see above) containing 1% NP-40. Following centrifugation at 15 000 r.p.m. for 10 min at 4°C, cell lysates were diluted to 0.5% NP-40 by addition of lysis buffer without NP-40. Cell lysates were cleared by sequential 45 min incubations at 4°C with preimmune TOR2 antisera (1:500 dilution) and 30 μl (packed volume) of protein A–Sepharose (PAS). TOR2 was immunoprecipitated by incubation with the TOR2-C–trpE antiserum (1:500 dilution) for 1 h at 4°C followed by incubation with 30 μl (packed volume) of PAS for 1 h. Immunocomplexes were washed four times in lysis buffer containing 0.5% NP-40, once with 50 mM Tris–HCl pH 7.5, 5 mM LiCl, and twice with PI kinase buffer (20 mM Tris–HCl pH 7.5, 100 mM NaCl, and 0.5 mM EGTA).

Immunoprecipitated TOR2 was resuspended in 25 μl of PI kinase buffer and reactions were started by addition of 25 μl of reaction buffer supplemented with 20 mM $MgCl_2$, 20 μM ATP, 10 μCi [γ-^{32}P]ATP, 10 μg sonicated PI (Sigma), and incubated for 15 min at 26°C. Under these conditions, the reaction was linear for up to 30 min. Where indicated, TOR2 immunoprecipitates were preincubated for 15 min at 4°C in 25 μl of PI kinase buffer containing 1 μM His6–FKBP12–rapamycin complex and PI kinase reactions were started as above. Reactions were stopped by addition of 80 μl of 1 M HCl. Following lipid extraction with 160 μl of chloroform:methanol (1:1 v/v), samples were analyzed with the borate TLC system, to resolve PI3P and PI4P (Walsh *et al.*, 1991), and autoradiography. Where indicated, following extraction, lipids were deacylated and fractionated by HPLC with a strong anion exchange column as described by Serunian *et al.* (1991). The [^{32}P]PI3P-labeled standard was produced by incubating [^{32}P]ATP and PI with PI3 kinase immunoprecipitated with anti-p85 antiserum (UBI) from insulin-stimulated rat fibroblasts overexpressing the insulin receptor (kindly provided by P.Blackshear). PI kinase activity was quantified with a phosphoimager.

Isolation of temperature-sensitive TOR2 mutants

Conditional alleles of the *TOR2* gene were isolated by *in vitro* chemical mutagenesis with hydroxylamine and plasmid shuffle (Sikorski and Boeke, 1991). Plasmid pML40-3 bearing the *TOR2* gene as a *Not*I cassette in the *CEN LEU2* plasmid pRS315 was mutagenized *in vitro* with 1 M hydroxylamine at 70°C for 60–135 min, purified by gel exclusion chromatography, and used to transform *E.coli* strain DH5α. Plasmid DNA was prepared, pooled and used to transform yeast strain MH346-1a (*Δtor2::ADE2 pSEY18-TOR2*) to leucine prototrophy at 24°C. Colonies that survived loss of the resident pSEY18-TOR2 plasmid at 24°C but not at 37°C were identified by replica plating to medium containing 5-fluoro orotic acid (5-FOA). Two independent, plasmid-linked ts mutants were identified that conferred temperature-sensitive growth on both minimal and rich (YPD) media. The ts mutations were mapped within the *TOR2* gene by demonstrating that the *Not*I cassette containing the *TOR2* gene subcloned into plasmid pRS315 conferred ts growth. For immunoprecipitations to detect TOR2 PI-4 kinase activity, the *TOR1* gene was disrupted in the MH346-1a strain (*Δtor2::ADE2*) bearing the wild-type *TOR2* gene or the *tor2-ts4* gene (on the *CEN LEU2 TOR2* plasmid pML40-3) by integration/disruption with plasmid pLW1 cleaved with *Xho*I, which bears a 3.9 kb internal *Bam*HI fragment of the *TOR1* gene cloned in the *URA3* integrating yeast vector YIplac211 (Gietz and Sugino, 1988).

FKBP12–rapamycin affinity chromatography

His6-tagged yeast FKBP12 protein was overproduced, purified and cross-linked to affigel-10 as previously described (Cardenas *et al.*, 1994b). The affigel–FKBP12 affinity matrix retained *cis–trans* peptidyl-prolyl isomerase activity that was inhibited by 1 μM FK506 or rapamycin, as assayed by the chymotrypsin-coupled cleavage of the chromogenic substrate, *N*-succ-ala-ala-pro-phe-*p*-nitroanilide (Heitman *et al.*, 1993).

Protein extracts were prepared by breaking cells with glass beads (60 OD_{600} units of cells/incubation) in 500 μl of lysis buffer containing 50 mM Tris–HCl pH 7.4, 0.5 M NaCl, 2 mM EDTA, 2 mM EGTA, 100 μM Na_3VO, 25 mM NaF, 25 mM β-glycerophosphate, 2 mM dithiothreitol (DTT), 1 mM benzamidine, 1 μg/ml pepstatin, 100 U/ml trasylol, 0.5 mM PMSF, supplemented with 1% Triton X-100, followed by centrifugation at 15 000 r.p.m. for 15 min. For binding reactions, the lysis buffer was diluted to give a final concentration of 160 mM NaCl and 0.3 % Triton X-100 and 30 μl packed volume of FKBP12–affigel-10, or affigel-10 beads, were added for each 1.5 ml incubation. Where indicated, binding reactions contained 1 μM rapamycin. Following incubation for 1 h at 4°C with gentle shaking, beads were washed four times with lysis buffer supplemented with 0.3% Triton X-100 and 200 mM NaCl, and twice with 10 mM Tris–HCl pH 7.4, 100 mM KCl. Bound material was eluted by boiling in SDS sample buffer and subjected to SDS–PAGE and Western blot analysis with the TOR2-C–trpE antiserum diluted 1:2000. Blots were developed using the ECL system (Amersham) according to the manufacturer's recommended instructions.

Cell cycle synchronization by α-factor and budding index determination

Cells of strain JK9-3da from a log phase culture (OD_{600} = 0.4–0.6) in YPD medium were collected by centrifugation at 1000 *g* and the

conditioned medium containing BAR1 protease was sterile filtered (Millipore 0.45 μM filters) and saved. Cells were transferred into fresh YPD medium preheated to 30°C containing 10 μg/ml synthetic α-factor and incubated at 30°C for 2 h. At this point, nearly 100% of cells were unbudded. Cells were collected as above, washed twice in fresh YPD medium, resuspended in conditioned YPD medium with or without 0.5 μg/ml rapamycin and incubated at 30°C for the times indicated in the legend to Figure 7. For budding index determinations, cells were briefly sonicated (5 s in a Branson water bath sonicator), applied to a hemocytometer and counted with a Nikon Labophot-2 microscope with 40× magnification. At least 200 cells were counted for each determination.

Indirect immunofluorescence and CDCFDA vital staining of yeast cells

Indirect immunofluorescence was performed using standard procedures (Pringle *et al.*, 1989). Briefly, yeast cells grown in 20 ml YPD medium to an OD_{600} = 0.5–1 were fixed with 4% paraformaldehyde (Sigma) for 1 h at 25°C with gentle shaking (Figure 3) or 2 h at 25°C and overnight at 4°C (Figure 8). Cells were collected by centrifugation at 1000 *g* for 5 min, washed twice in phosphate-buffered saline (PBS; 20 mM $NaPO_4$ pH 7.5, 20 mM NaCl), resuspended in 2–4 ml of 100 mM KPO_4 pH 7.5, 1.2 M sorbitol, 20 mM β-mercaptoethanol, and incubated for 10 min at 30°C. Following collection as above, cells were resuspended in 2–4 ml of 1.2 M sorbitol, 100 mM KPO_4 pH 7.5, supplemented with 3500 U/ml oxalyticase and spheroplasted by incubating at 30°C for 20 min. Spheroplasts were pelleted at 800 *g* for 4 min, washed three times with 15 ml of 1.2 M sorbitol, 100 mM KPO_4 pH 7.5 and resuspended in 200–500 μl of the same buffer. Spheroplasts were immobilized on polylysine-coated slides. For data shown in Figure 3, spheroplasts were further permeabilized by immersion in methanol at –20°C for 6 min, and acetone at –20°C for 30 s. Immobilized spheroplasts were incubated with anti-TOR2 peptide antiserum [preabsorbed on paraformaldehyde-fixed whole yeast cells, and diluted 1:50 in NTSB (PBS containing 0.1% Triton X-100, 0.02% SDS, and 10 mg/ml BSA)] for 1 h at 30°C. Following three washes in PBS containing 5 mg/ml BSA, anti-rabbit-dichlorotriazinyl amino fluorescein (DTAF) diluted 1:100 in NTSB was added for 45 min at 30°C. Finally, slides were washed three times in NTSB. For experiments presented in Figure 8, the methanol–acetone step was omitted and all detergents were eliminated in buffers for antibody decoration. Slides were mounted in Vertex mounting media containing 2 μg/ml of DAPI. Immunofluorescence was recorded with a Nikon Optiphot-2 fluorescence microscope equipped with Nikon filters DM510, DM400 and DM580 and a Nikon FX-35DX 35 mm camera. The same fields of cells were also analyzed by Nomarski optics.

CDCFDA vital staining was performed exactly as indicated by Roberts *et al.* (1991) and monitored by immunofluorescence as above.

Vacuole preparation and lipid extraction

Vacuoles were prepared essentially as described by Conradt *et al.* (1992). Cells were harvested at 1000 *g* for 5 min. Cell pellets were gently resuspended in 5 ml of 100 mM PIPES–KOH pH 9.4, 10 mM DTT, and incubated for 10 min at 30°C with gentle shaking. Following centrifugation as above, cells were resuspended in 5 ml of YPD, 0.6 M sorbitol, 10 mM DTT, 50 mM KPO_4, pH 7.5, and spheroplasted by addition of 3500 U/ml oxalyticase (Enzogenetics) for 20 min at 30°C. Spheroplasts were collected by centrifugation at 1000 *g* for 4 min and 1500 *g* for 1 min at 4°C. Spheroplasts were lysed by gentle resuspension in 0.9 ml of ice-cold 10% Ficoll, 0.2 M sorbitol, 10 mM PIPES–KOH pH 6.8 supplemented with 8 μg/ml DEAE–dextran, and the protease inhibitors as indicated above for cell lysis buffer. For vacuole isolation, 2 ml of lysate were transferred to an ultraclear SW41 tube (Beckman) and overlayed with 4 ml of 8% Ficoll, 3 ml of 4% Ficoll and 2 ml of 0% Ficoll (made in 10 mM PIPES–KOH pH 6.8, 0.2 M sorbitol). The gradient was centrifuged at 110 000 *g* for 90 min at 4°C, vacuoles were collected in 500 μl from the 4–0% Ficoll interface.

At this point, aliquots from the total spheroplast lysate and vacuolar fraction were taken for protein determination using the BioRad protein microassay. For PI kinase assays, samples containing 3 mg of protein from the total spheroplast lysate and vacuolar fraction were made 1% with NP-40 and immunoprecipitated with the anti-TOR2-C–trpE antisera as described above. For Western blot analysis, samples from the total cell lysate and the vacuolar fraction were precipitated with 20% trichloroacetic acid at 4°C for 2 h. Protein pellets were recovered by centrifugation at 15 000 r.p.m. in a microcentrifuge at 4°C and resuspended in 100 mM Tris–HCl, pH 11, 3% SDS, 100 mM DTT, 15% glycerol and neutralized with 1.5 M Tris–HCl, pH 8.8 as required. Samples with 40 μg of protein were analyzed by Western blot with antisera against the TOR2-C–trpE fusion protein, two subunits of the vacuolar H^+-ATPase (VPH1 and VMA2) and the cytosolic protein FKBP12.

Acknowledgements

We thank R.Scott Muir for truly superb technical assistance, Liping Wang for technical assistance, Mike Lorenz for strains and MIC determinations, Mike Hall, Alex Tzagoloff, Eric Kuebler, Perry Blackshear and Tom Stevens for materials, the Drug Synthesis and Chemistry Branch of the National Cancer Institute for rapamycin, Phillip Majerus and Scott Emr for advice, Joe Nevins for support and comments, Ann-Marie Pendergast for comments and Sandra Bowling for manuscript preparation. Supported in part by grants PO1 HL50985-01 (NIH) and grant #4050 (Council for Tobacco Research) to Maria Cardenas. Joseph Heitman is an investigator of the Howard Hughes Medical Institute.

References

Aitken,J.F., van Heusden,G.P.H., Temkin,M. and Dowhan,W. (1990) The gene encoding the phosphatidylinositol transfer protein is essential for cell growth. *J. Biol. Chem.*, **265**, 4711–4717.

Albers,M.W., Williams,R.T., Brown,E.J., Tanaka,A., Hall,F.L. and Schreiber,S.L. (1993) FKBP–rapamycin inhibits a cyclin-dependent kinase activity and a cyclin D1–Cdk association in early G1 of an osteosarcoma cell line. *J. Biol. Chem.*, **268**, 22825–22829.

Bankaitis,V.,A., Aitken,J., Cleves,A.E. and Dowhan,W. (1990) An essential role for a phospholipid transfer protein in yeast Golgi function. *Nature*, **347**, 561–562.

Becker,G.W. and Lester,R.L. (1977) Changes in phospholipids of *Saccharomyces cerevisiae* associated with inositol-less death. *J. Biol. Chem.*, **252**, 8684–8691.

Berridge,M.J. (1993) Inositol trisphosphate and calcium signalling. *Nature*, **361**, 315–325.

Berridge,M.J. and Irvine,R.F. (1989) Inositol phosphates and cell signalling. *Nature*, **341**, 197–205.

Bierer,B.E., Mattila,P.S., Standaert,R.F., Herzenberg,L.A., Burakoff,S.J., Crabtree,G. and Schreiber,S.L. (1990) Two distinct signal transmission pathways in T lymphocytes are inhibited by complexes formed between an immunophilin and either FK506 or rapamycin. *Proc. Natl Acad. Sci. USA*, **87**, 9231–9235.

Boronenkov,I.V. and Anderson,R.F. (1995) The sequence of phosphatidylinositol-4-phosphate 5-kinase defines a novel family of lipid kinases. *J. Biol. Chem.*, **270**, 2881–2884.

Breuder,T., Hemenway,C.S., Movva,N.R., Cardenas,M.E. and Heitman,J. (1994) Calcineurin is essential in cyclosporin A- and FK506-sensitive yeast strains. *Proc. Natl Acad. Sci. USA*, **91**, 5372–5376.

Brown,E.J., Albers,M.W., Shin,T.B., Ichikawa,K., Keith,C.T., Lane,W.S. and Schreiber,S.L. (1994) A mammalian protein targeted by G1-arresting rapamycin–receptor complex. *Nature*, **369**, 756–759.

Cafferkey,R., Young,P.R., McLaughlin,M.M., Bergsma,D.J., Koltin,Y., Sathe,G.M., Faucette,L., Eng,W.-K., Johnson,R.K. and Livi,G.P. (1993) Dominant missense mutations in a novel yeast protein related to mammalian phosphatidylinositol 3-kinase and VPS34 abrogate rapamycin cytotoxicity. *Mol. Cell. Biol.*, **13**, 6012–6023.

Cardenas,M.E., Laroche,T. and Gasser,S.M. (1990) The composition and morphology of yeast nuclear scaffolds. *J. Cell Sci.*, **96**, 439–450.

Cardenas,M.E., Lorenz,M., Hemenway,C. and Heitman,J. (1994a) Yeast as model-T cells. *Perspect. Drug Discovery Design*, **2**, 103–126.

Cardenas,M., Hemenway,C., Muir,R.S., Ye,R., Fiorentino,D. and Heitman,J. (1994b) Immunophilins interact with calcineurin in the absence of exogenous immunosuppressive ligands. *EMBO J.*, **13**, 5944–5957.

Cardenas,M., Muir,R.S., Breuder,T. and Heitman,J. (1995) Targets of immunophilin–immunosuppressant complexes are distinct highly conserved regions of calcineurin A. *EMBO J.*, **14**, 2772–2783.

Chiu,M.I., Katz,H. and Berlin,V. (1994) RAPT1, a mammalian homolog of yeast Tor, interacts with the FKBP12/rapamycin complex. *Proc. Natl Acad. Sci. USA*, **91**, 12574–12578.

Chung,J., Kuo,C.J., Crabtree,G.R. and Blenis,J. (1992) Rapamycin–FKBP specifically blocks growth-dependent activation of and signaling by the 70 kDa S6 protein kinases. *Cell*, **69**, 1227–1236.

Clipstone,N.A. and Crabtree,G.R. (1992) Identification of calcineurin as a key signalling enzyme in T-lymphocyte activation. *Nature*, **357**, 695–697.

Conradt,B., Shaw,J., Vida,T., Emr,S. and Wickner,W. (1992) *In vitro* reactions of vacuole inheritance in *Saccharomyces cerevisiae*. *J. Cell Biol.*, **119**, 1469–1479.

Cyert,M.S., Kunisawa,R., Kaim,D. and Thorner,J. (1991) Yeast has homologs (*CNA1* and *CNA2* gene products) of mammalian calcineurin, a calmodulin-regulated phosphoprotein phosphatase. *Proc. Natl Acad. Sci. USA*, **88**, 7376–7380.

Dahl,C., Biemann,H.-P. and Dahl,J. (1987) A protein kinase antigenically related to $pp60^{v\text{-}src}$ possibly involved in yeast cell cycle control: positive *in vivo* regulation by sterol. *Proc. Natl Acad. Sci. USA*, **84**, 4012–4016.

Dahl,J.S. and Dahl,C.E. (1985) Stimulation of cell proliferation and polyphosphoinositide metabolism in *Saccharomyces cerevisiae* GL7 by ergosterol. *Biochem. Biophy. Res. Commun.*, **133**, 844–850.

de Groot,R.P., Ballou,L.M. and Sassone-Corsi,P. (1994) Positive regulation of the cAMP-responsive activator CREM by the p70 S6 kinase: an alternative route to mitogen-induced gene expression. *Cell*, **79**, 81–91.

Dilling,M.B., Dias,P., Shapiro,D.N., Germain,G.S., Johnson,R.K. and Houghton,P.J. (1994) Rapamycin selectively inhibits the growth of childhood rhabdomyosarcoma cells through inhibition of signaling via the type I insulin-like growth factor receptor. *Cancer Res.*, **54**, 903–907.

Dulic,V. and Riezman,H. (1989) Characterization of the *END1* gene required for vacuole biogenesis and gluconeogenic growth of budding yeast. *EMBO J.*, **8**, 1349–1359.

Dumont,F.L., Staruch,M.J., Koprak,S.L., Melino,M.R. and Sigal,N.H. (1990a) Distinct mechanisms of suppression of murine T cell activation by the related macrolides FK506 and rapamycin. *J. Immunol.*, **144**, 251–258.

Dumont,F.J., Melino,M.R., Staruch,M.J., Koprak,S.L., Fischer,P.A. and Sigal,N.H. (1990b) The immunosuppressive macrolides FK-506 and rapamycin act as reciprocal antagonists in murine T-cells. *J. Immunol.*, **144**, 1418–1424.

Flanagan,C.A., Schnieders,E.A., Emerick,A.W., Kunisawa,R., Admon,A. and Thorner,J. (1993) Phosphatidylinositol 4-kinase: gene structure and requirement for yeast cell viability. *Science*, **262**, 1444–1448.

Foor,F., Parent,S.A., Morin,N., Dahl,A.M., Ramadan,N., Chrebet,G., Bostian,K.A. and Nielsen,J.B. (1992) Calcineurin mediates inhibition by FK506 and cyclosporin of recovery from α-factor arrest in yeast. *Nature*, **360**, 682–684.

Garcia-Bustos,J.F., Marini,F., Stevenson,I., Frei,C. and Hall,M.N. (1994) PIK1, an essential phosphatidylinositol 4-kinase associated with the yeast nucleus. *EMBO J.*, **13**, 2352–2361.

Gietz,R.D. and Sugino,A. (1988) New yeast–*Escherichia coli* shuttle vectors constructed with *in vitro* mutagenized yeast genes lacking six-base pair restriction sites. *Gene*, **74**, 527–534.

Goldschmidt-Clermont,P.J., Machesky,L.M., Baldassare,J.J. and Pollard,T.D. (1990) The actin-binding protein profilin binds to PIP_2 and inhibits its hydrolysis by phospholipase C. *Science*, **247**, 1575–1578.

Harlow,E. and Lane,D. (1988) *Antibodies. A Laboratory Manual*. Cold Spring Harbor Laboratory Press, Cold Spring Harbor, NY.

Hawkins,P.T., Stephens,L.R. and Piggott,J.R. (1993) Analysis of inositol metabolites produced by *Saccharomyces cerevisiae* in response to glucose stimulation. *J. Biol. Chem.*, **268**, 3374–3383.

Hay,J.C., Fisette,P.L., Jenkins,G.H., Fukami,K., Takenawa,T., Anderson, R.A. and Martin,T.F.J. (1995) ATP-dependent inositide phosphorylation required for Ca^{2+}-activated secretion. *Nature*, **374**, 173–177.

Heitman,J., Movva,N.R. and Hall,M.N. (1991a) Targets for cell cycle arrest by the immunosuppressant rapamycin in yeast. *Science*, **253**, 905–909.

Heitman,J., Movva,N.R., Hiestand,P.C. and Hall,M.N. (1991b) FK506-binding protein proline rotamase is a target for the immunosuppressive agent FK506 in *Saccharomyces cerevisiae*. *Proc. Natl Acad. Sci. USA*, **88**, 1948–1952.

Heitman,J., Movva,N.R. and Hall,M.N. (1992) Proline isomerases at the crossroads of protein folding, signal transduction, and immunosuppression. *New Biol.*, **4**, 448–460.

Heitman,J., Koller,A., Cardenas,M.E. and Hall,M.N. (1993) Identification of immunosuppressive drug targets in yeast. *Methods*, **5**, 176–187.

Helliwell,S.B., Wagner,P., Kunz,J., Deuter-Reinhard,M., Henriquez,R. and Hall,M.N. (1994) TOR1 and TOR2 are structurally and functionally similar but not identical phosphatidylinositol kinase homologues in yeast. *Mol. Biol. Cell*, **5**, 105–118.

Hiles,I.D., Otsu,M., Volinia,S., Fry,M.J., Gout,I., Dhand,R., Panayotou,G., Ruiz-Larrea,F., Thompson,A., Totty,N.F., Hsuan,J.J., Courtneidge,S.A., Parker,P.J. and Waterfield,M.D. (1992) Phosphatidylinositol 3-kinase: structure and expression of the 110 kDa catalytic subunit. *Cell*, **70**, 419–429.

Ho,S.N., Hunt,H.D., Horton,R.M., Pullen,J.K. and Pease,L.R. (1989) Site-directed mutagenesis by overlap extension using the polymerase chain reaction. *Gene*, **77**, 51–59.

Janmey,P.A. (1994) Phosphoinositides and calcium as regulators of cellular actin assembly and disassembly. *Annu. Rev. Physiol.*, **56**, 169–191.

Janmey,P.A. (1995) Protein regulation by phosphatidylinositol lipids. *Chem. Biol.*, **2**, 61–65.

Janmey,P.A. and Stossel,T.P. (1987) Modulation of gelsolin function by phosphatidylinositol 4,5-bisphosphate. *Nature*, **325**, 362–364.

Jayaraman,T. and Marks,A.R. (1993) Rapamycin–FKBP12 blocks proliferation, induces differentation, and inhibits cdc2 kinase activity in a myogenic cell line. *J. Biol. Chem.*, **268**, 25385–25388.

Kapeller,R. and Cantley,L.C. (1994) Phosphatidylinositol 3-kinase. *BioEssays*, **16**, 565–576.

Kato,R. and Ogawa,H. (1994) An essential gene, *ESR1*, is required for mitotic cell growth, DNA repair and meiotic recombination in *Saccharomyces cerevisiae*. *Nucleic Acids Res.*, **22**, 3104–3112.

Klionsky,D., Herman,P.K. and Emr,S.D. (1990) The fungal vacuole: composition, function, and biogenesis. *Microbiol. Rev.*, **54**, 266–292.

Knighton,D.R., Zheng,J., Eyck,L.F.T., Ashford,V.A., Xuong,N.-H., Taylor,S.S. and Sowadski,J.M. (1991) Crystal structure of the catalytic subunit of cyclic adenosine monophosphate-dependent protein kinase. *Science*, **253**, 407–413.

Koerner,T.J., Hill,J.E., Myers,A.M. and Tzagoloff,A. (1991) High-expression vectors with multiple cloning sites for construction of *trpE* fusion genes: pATH vectors. *Methods Enzymol.*, **194**, 477–490.

Koltin,Y., Faucette,L., Bergsma,D.J., Levy,M.A., Cafferkey,R., Koser,P.L., Johnson,R.K. and Livi,G.P. (1991) Rapamycin sensitivity in *Saccharomyces cerevisiae* is mediated by a peptidyl-prolyl *cis–trans* isomerase related to human FK506-binding protein. *Mol. Cell. Biol.*, **11**, 1718–1723.

Kunz,J., Henriquez,R., Schneider,U., Deuter-Reinhard,M., Movva,N.R. and Hall,M.N. (1993) Target of rapamycin in yeast, TOR2, is an essential phosphatidylinositol kinase homolog required for G_1 progression. *Cell*, **73**, 585–596.

Liu,J. (1993) FK506 and cyclosporin, molecular probes for studying intracellular signal transduction. *Immunol. Today*, **14**, 290–295.

Liu,J., Farmer,J.D., Lane,W.S., Friedman,J., Weissman,I. and Schreiber,S.L. (1991) Calcineurin is a common target of cyclophilin–cyclosporin A and FKBP–FK506 complexes. *Cell*, **66**, 807–815.

Liu,J., Albers,M.W., Wandless,T.J., Luan,S., Alberg,D.G., Belshaw,P.J., Cohen,P., MacKintosh,C., Klee,C.B. and Schreiber,S.L. (1992) Inhibition of T cell signaling by immunophilin–ligand complexes correlates with loss of calcineurin phosphatase activity. *Biochemistry*, **31**, 3896–3901.

Liu,Y., Ishii,S., Tokai,M., Tsutsumi,H., Ohki,O., Akade,R., Tanaka,K., Tsuchiya,E., Fukui,S. and Miyakawa,T. (1991) The *Saccharomyces cerevisiae* genes (*CMP1* and *CMP2*) encoding calmodulin-binding proteins homologous to the catalytic subunit of mammalian protein phosphatase 2B. *Mol. Gen. Genet.*, **227**, 52–59.

Majerus,P.W., Ross,T.S., Cunningham,T.W., Caldwell,K.K., Jefferson, A.B. and Bansal,V.S. (1990) Recent insights in phosphatidylinositol signaling. *Cell*, **63**, 459–465.

Mattila,P.S., Ullman,K.S., Fiering,S., McCutcheon,M., Crabtree,G.R. and Herzenberg,L.A. (1990) The actions of cyclosporin A and FK506 suggest a novel step in the activation of T lymphocytes. *EMBO J.*, **9**, 4425–4433.

Nakamura,T., Liu,Y., Hirata,D., Namba,H., Harada,S.-i., Hirokawa,T. and Miyakawa,T. (1993) Protein phosphatase type 2B (calcineurin)-mediated, FK506-sensitive regulation of intracellular ions in yeast is an important determinant for adaptation to high salt stress conditions. *EMBO J.*, **12**, 4063–4071.

Nickels,J.T.J. and Carman,G.M. (1993) Photoaffinity labeling of the 45-kDa and 55-kDa forms of phosphatidylinositol 4-kinase from the yeast *Saccharomyces cerevisiae*. *J. Biol. Chem.*, **268**, 24083–24088.

Nikawa,J.-i., Kodaki,T. and Yamashita,S. (1987) Primary structure and disruption of the phosphatidylinositol synthase gene of *Saccharomyces cerevisiae*. *J. Biol. Chem.*, **262**, 4876–4881.

Novick,P., Osmond,B.C. and Botstein,D. (1989) Suppressors of yeast actin mutations. *Genetics*, **121**, 659–674.

O'Keefe,S.J., Tamura,J.i., Kincaid,R.L., Tocci,M.J. and O'Neill,E.A. (1992) FK-506- and CsA-sensitive activation of the interleukin-2 promoter by calcineurin. *Nature*, **357**, 692–694.

Paltauf,F., Kohlwein,S.D. and Henry,S.A. (1992) Regulation and

compartmentalization of lipid synthesis in yeast. In Jones,E., Pringle,J. and Broach,J. (eds), *The Molecular and Cellular Biology of the Yeast Saccharomyces*. Cold Spring Harbor Laboratory Press, Cold Spring Harbor, NY, Vol. 2, pp. 415–500.

Price,D.J., Grove,J.R., Calvo,V., Avruch,J. and Bierer,B.E. (1992) Rapamycin-induced inhibition of the 70-kilodalton S6 protein kinase. *Science*, **257**, 973–977.

Pringle,J.R., Preston,R.A., Adams,A.E.M., Stearns,T., Drubin,D.G., Haarer,B.K. and Jones,E.W. (1989) Fluorescence microscopy methods for yeast. *Methods Cell Biol.*, **31**, 357–435.

Raymond,C.K., O'Hara,P.J., Eichinger,G., Rothman,J.H. and Stevens,T.H. (1990) Molecular analysis of the yeast *VPS3* gene and the role of its product in vacuolar protein sorting and vascular segregation during the cell cycle. *J. Cell Biol.*, **111**, 877–892.

Raymond,C.K., Howard-Stevenson,I., Vater,C.A. and Stevens,T.H. (1992) Morphological classification of the yeast vacuolar protein sorting mutants: evidence for a prevacuolar compartment in class E *vps* mutants. *Mol. Biol. Cell*, **3**, 1389–1402.

Roberts,C.J., Raymond,C.K., Yamashiro,C.T. and Stevens,T.H. (1991) Methods for studying the yeast vacuole. *Methods Enzymol.*, **194**, 644–661.

Sabatini,D.M., Erdjument-Bromage,H., Lui,M., Tempst,P. and Snyder,S.H. (1994) RAFT1: a mammalian protein that binds to FKBP12 in a rapamycin-dependent fashion and is homologous to yeast TORs. *Cell*, **78**, 35–43.

Sabers,C.J., Martin,M.M., Brunn,G.J., Williams,J.M., Dumont,F.J., Wiederrecht,G. and Abraham,R.T. (1995) Isolation of a protein target of the FKBP12–rapamycin complex in mammalian cells. *J. Biol. Chem.*, **270**, 815–822.

Schomerus,C. and Kuntzel,H. (1992) CDC25-dependent induction of inositol 1,4,5- trisphosphate and diacylglycerol in *Saccharomyces cerevisiae* by nitrogen. *FEBS Lett.*, **307**, 249–252.

Schreiber,S.L. (1991) Chemistry and biology of the immunophilins and their immunosuppressive ligands. *Science*, **251**, 283–287.

Schreiber,S.L. and Crabtree,G.R. (1992) The mechanism of action of cyclosporin A and FK506. *Immunol. Today*, **13**, 136–142.

Schu,P.V., Takegawa,K., Fry,M.J., Stack,J.H., Waterfield,M.D. and Emr,S.D. (1993) Phosphatidylinositol 3-kinase encoded by yeast *VPS34* gene essential for protein sorting. *Science*, **260**, 88–91.

Serrano,R. (1988) Structure and function of proton translocating ATPase in the plasma membrane of plants and fungi. *Biochim. Biophys. Acta*, **947**, 1–28.

Serunian,L.A., Auger,K.R. and Cantley,L.C. (1991) Identification and quantification of polyphosphoinositides produced in response to platelet-derived growth factor stimulation. *Methods Enzymol.*, **198**, 78–87.

Sheetz,M.P. and Singer,S.J. (1974) Biological membranes as bilayer couples. A molecular mechanism of drug–erythrocyte interactions. *Proc. Natl Acad. Sci. USA*, **71**, 4457–4461.

Sikorski,R.S. and Boeke,J.D. (1991) *In vitro* mutagenesis and plasmid shuffling: from cloned gene to mutant yeast. *Methods Enzymol.*, **194**, 302–318.

Stack,J.H., Herman, P.K., Schu,P.V. and Emr,S.D. (1993) A membrane-associated complex containing the Vps15 protein kinase and the Vps34 PI 3-kinase is essential for protein sorting to the yeast lysosome-like vacuole. *EMBO J.*, **12**, 2195–2204.

Sylvia,V., Curtin,G., Norman,J., Stec,J. and Busbee,D. (1988) Activation of a low specific activity form of DNA polymerase α by inositol-1,4-bisphosphate. *Cell*, **54**, 651–658.

Uno,I., Fukami,K., Kato,H., Takenawa,T. and Ishikawa,T. (1988) Essential role for phosphatidylinositol 4,5-bisphosphate in yeast cell proliferation. *Nature*, **333**, 188–190.

Walsh,J.P., Caldwell,K.K. and Majerus,P.W. (1991) Formation of phosphatidylinositol 3-phosphate by isomerization from phosphatidyl-inositol 4-phosphate. *Proc. Natl Acad. Sci. USA*, **88**, 9184–9187.

Weisman,L.S. and Wickner,W. (1988) Intervacuole exchange in the yeast zygote: a new pathway in organelle communication. *Science*, **241**, 589–591.

Wong,K. and Cantley,L.C. (1994) Cloning and characterization of a human phosphatidylinositol 4-kinase. *J. Biol. Chem.*, **269**, 28878–28884.

Yamamoto,A., DeWald,d.B., Boronenkov,I.V., Anderson,R.A., Emr,S.D. and Koshland,D. (1995) Novel PI(4) 5-kinase homolog, Fab1p, essential for normal vacuolar function and morphology in yeast. *Mol. Biol. Cell*, **6**, 525–539.

Ye,R.R. and Bretscher,A. (1992) Identification and molecular characterization of the calmodulin-binding subunit gene (*CMP1*) of protein phosphatase 2B from *Saccharomyces cerevisiae*. *Eur. J. Biochem.*, **204**, 713–723.

York,J.D., Saffitz,J.E. and Majerus,P.W. (1994) Inositol polyphosphate 1-phosphatase is present in the nucleus and inhibits DNA synthesis. *J. Biol. Chem.*, **269**, 19992–19999.

Yoshida,S., Ohya,Y., Goebl,M., Nakano,A. and Anraku,Y. (1994) A novel gene, *STT4*, encodes a phosphatidylinositol 4-kinase in the *PKC1* protein kinase pathway of *Saccharomyces cerevisiae*. *J. Biol. Chem.*, **269**, 1166–1171.

Received on May 26, 1995